1970

Magnetohydrodynamic stability of laminar flow in the entrance region of a parallel-plate channel

Thomas Eldon Eaton

Department:

MAGNETOHYDRODYNAMIC STABILITY OF LAMINAR FLOW IN THE ENTRANCE REGION OF A PARALLEL-PLATE CHANNEL

BY

THOMAS ELDON EATON, 1948-

A

THESIS

submitted to the faculty of

THE UNIVERSITY OF MISSOURI-ROLLA

in partial fulfillment of the requirements for the

Degree of

MASTER OF SCIENCE IN MECHANICAL ENGINEERING

Rolla, Missouri

1970

Approved by

T. S. Chen (advisor) A. L. Crosbie

Xavier R Avula

ABSTRACT

The hydrodynamic stability of laminar flow of an electrically conducting fluid flowing in a parallel-plate channel with an applied transverse magnetic field is investigated. The linear perturbation theory of hydrodynamic stability along with the assumption of low magnetic Reynolds number is applied to the governing equations to derive the governing magnetohydrodynamic stability equation. A finite difference scheme is employed to numerically solve the magnetohydrodynamic stability equation. Neutral stability characteristics of the flow in the entrance region are obtained and presented. The neutral stability characteristics of the fully developed Hartmann flow are also re-examined and compared with those of a previous investigation which utilizes an analytical method of solution. A linearized velocity solution for developing flow is used in the stability calculations.

The numerically determined neutral stability results for the fully developed Hartmann flow are in excellent agreement with those of the analytical solution. The results presented here for Hartmann flow are believed to be more accurate owing to the more exact nature of the numerical solution.

It is found that the critical Reynolds number for the developing flow induced by the uniform inlet velocity profile decreases rapidly with axial distance in the entrance region and monotonically approaches the fully developed value at large axial distances. For Hartmann numbers of less than 2, the decrease is monotonic; however, for larger Hartmann numbers, the critical Reynolds number decreases rapidly and goes below that of the fully developed Hartmann flow somewhere in the entrance region of the channel and then approaches this fully developed value monotonically from below at large axial distances.

The critical Reynolds number for the developing flow induced by a parabolic inlet velocity profile approaches the fully developed critical Reynolds number monotonically from a value of 3850 at the inlet for Hartmann numbers of less than 2. For larger Hartmann numbers, the critical Reynolds number over-shoots the fully developed value, approaching it monotonically from above at large axial distances.

ACKNOWLEDGEMENT

The author wishes to express his most sincere gratitude to Professor Ta-Shen Chen for his assistance, advice, and encouragement in this work. Professor Chen has continuously provided vital recommendations and criticisms throughout the investigation.

The author is also indebted to Mr. Gwok-Liang Chen and to Mr. Lung-Mau Huang for many discussions concerning the computational aspects of the present investigation. The support of the computational expenses by the Mechanical Engineering Department of the University of Missouri-Rolla is gratefully asknowledged.

The author would like to thank Mrs. Connie Hendrix for typing the manuscript.

Finally, the author gratefully acknowledges the National Science Foundation for the financial support received during this educational endeavor.

TABLE OF CONTENTS

TABLE OF CONTENTS (Continued)

LIST OF FIGURES

LIST OF TABLES

NOMENCLATURE

$\bar{a}_1, \bar{a}_2, \bar{a}_3$	elements of matrix [B], Equation (38)
a_1, a_2, a_3	real part of elements of Matrix [A], Equation (40)
$\vec{B}$	magnetic field vector
b_1, b_2, b_3	imaginary part of elements of matrix [A], Equation (40)
c	wave velocity of disturbances
$\vec{E}$	electric field vector
g	discrete value of the transformed function of ϕ
$\vec{H}$	magnetic field vector
H_o	applied magnetic field normal to the flow
h	ratio of induced to applied magnetic field, H_x/H_o
h_x^+	perturbed axial magnetic field
h_y^+	perturbed transverse magnetic field
$\vec{J}$	electrical current density vector
L	channel half-height
M	Hartmann number, $\mu_m H_o L(\sigma/u_f)^{1/2}$
N	number of steps in finite difference mesh
p	resultant pressure
$\bar{p}$	pressure of main flow
p^+	perturbation pressure
R	Reynolds number, LU/ν
R_m	magnetic Reynolds number, LU/λ
r	finite difference mesh size or step size
t	dimensionless time, t*U/L

NOMENCLATURE (Continued)

t^*	dimensional time
u	resultant axial velocity component
$\bar{u}$	axial velocity component of main flow
u^+	perturbed axial velocity
U	average axial velocity
$\vec{V}$	velocity vector
v	resultant transverse velocity component
$\bar{v}$	transverse velocity component of main flow
v^+	perturbed transverse velocity
W	dimensionless axial velocity, u/U
$\bar{x}$	dimensional stretched axial coordinate
$\bar{X}$	dimensionless stretched axial coordinate, $(\bar{x}/L)/R$
x^*	dimensional axial coordinate
X	dimensionless axial coordinate, $(x^*/L)/R$
y^*	dimensional transverse coordinate
y	dimensionless transverse coordinate, y^*/L
∇	the del operator
$\vec{\nabla}$	gradient
∇^2	the Laplacian operator
α	dimensionless wave number
$\bar{\alpha}$	dimensional wave number
α_i	eigenvalues of $\alpha_i = \tan \alpha_i$
δ	central difference operator
$\varepsilon(M,\bar{X})$	weighting function, Equation (13)

NOMENCLATURE (Continued)

θ	dimensionless amplitude function of magnetic perturbation, θ^*/LH_o
θ^*	dimensional amplitude function of magnetic perturbation
λ	a constant, $1/\mu_m\sigma$
μ	averaging operator
μ_m	magnetic permeability
μ_f	absolute or dynamic fluid viscosity
ρ	fluid density
σ	electrical conductivity
$\emptyset$	dimensionless amplitude function of velocity perturbation, $\emptyset^*/LU$
$\emptyset^*$	dimensional amplitude function of velocity perturbation
χ	dimensionless magnetic stream function, χ^*/LH_o
χ^*	dimensional magnetic stream function
Ψ	dimensionless fluid stream function, Ψ^*/LU
Ψ^*	dimensional fluid stream function

Superscripts

','',''',iv	derivatives with respect to y
-	main flow component
*	dimensional quantity
+	perturbation quantity
$\rightarrow$	vector quantity
$\hat{}$	unit vector - $\hat{i}$, $\hat{j}$, $\hat{k}$ = unit vectors for x*,y*,z*, respectively

NOMENCLATURE (Continued)

Subscripts

crit	critical condition
fd	fully developed condition
o	condition at channel inlet
x,y	x*,y* -component

I. INTRODUCTION

A. General Background

Within the twentieth century, the areas of magnetohydrodynamics and hydrodynamic stability have been born and rigorously investigated. Magnetohydrodynamics (MHD) is a rather complicated science which deals with the coupled problems of fluid mechanics and electromagnetics. MHD utilizes the fluid continuum model to approach this coupled problem while plasma dynamics employs the statistical model to deal with the coupled analysis. The coupling factor between fluid mechanics and electromagnetics is the electrical conduction property of the fluid. A conductor moving perpendicular to a magnetic field creates a current perpendicular to the direction of the fluid motion and to the direction of the magnetic field; furthermore, motion of the fluid perpendicular to the magnetic field is opposed by an induced electromotive force, the MHD body or field force.

The linear theory of hydrodynamic stability predicts the response of laminar fluid flow to small disturbances. Basically, perturbations or small disturbances are superimposed onto the main flow in the governing equations. If the analysis of the perturbation equations shows that these disturbances grow with time, the flow is "theoretically unstable" to small disturbances. If the analysis

shows the disturbance to decay with time, the flow is "theoretically stable" to small disturbances. When the disturbances neither grow nor decay, the flow is said to be neutrally stable. In actual flow, the critical Reynolds number is the minimum Reynolds number at which the laminar flow becomes unstable. Once this Reynolds number is exceeded, the flow may change to another laminar flow pattern or begin its transition to turbulent flow. Further, the theoretically determined critical Reynolds number is lower or more conservative than the experimentally observed critical Reynolds number. More detailed introductory remarks on the stability of laminar flow can be found, for example, in a book by Schlichting (1).

The presence of the MHD body force, which may be quite large relative to more common body forces such as gravity or acceleration, creates an interesting hydrodynamic stability problem. One would expect that the presence of a magnetic field force tends to increase the stability of laminar flows to small disturbances; for the reason that the field force will essentially "tense-up" the flow to changes of any nature. Utilizing the concept of disturbance energy, one might say that the field force greatly enhances the dissipation of any disturbance energy. This combined problem of hydrodynamic stability and magnetohydrodynamics will be referred to as magnetohydrodynamic

stability by the author; although, hydromagnetic or magnetofluidmechanic stability might have been chosen. The latter would better represent the topic; however, the former is a conventional misnomer.

The linear perturbation theory of magnetohydrodynamic stability consists of perturbing (disturbing) all main quantities of the flow and magnetic fields, neglecting the products of small perturbation quantities (linearizing), and analyzing the equations due to perturbation terms. The perturbations for the flow and magnetic fields are then represented, respectively, as a spatially dependent amplitude function multiplied by a time and space dependent exponential which constitutes the respective perturbation stream function. These perturbation stream functions, in turn, satisfy conservation of mass and of magnetic field, respectively. With the perturbations in this form, one may predict the growth or decay of the disturbances with time and thus the relative instability or stability of the laminar fluid motion under a magnetic field. Another obvious case of importance is the neutral stability of laminar flow; the condition at which the flow is neither stable nor unstable. Under this condition, laminar flow is on the threshold of the change to other flow patterns.

B. Previous Studies

Several investigations on the MHD stability problems for the fully developed flow in a channel have appeared in the literature. Of these, the work of Stuart (2) and of Lock (3) will be mentioned briefly. Stuart (2) investigated the MHD stability of a conducting fluid moving parallel to the magnetic field in a parallel-plate channel. With this scheme, no changes in the velocity profile due to the magnetic field are experienced. Stuart found that the magnetic field affects the perturbations such that the stability of flow is increased; an effect which is substantial only for very large Hartmann numbers.

Lock (3) investigated the case where the conducting fluid moved perpendicular to the magnetic field for the parallel-plate duct geometry. Perhaps Lock's most significant finding is that the main effect of the magnetic field on the stability problem is reflected in the changes in the velocity profiles due to the presence of the MHD body force. Indeed, in his stability calculations, Lock neglected all terms involving the magnetic field except the velocity profiles corresponding to the fully developed Hartmann flow. Lock found that the critical Reynolds number increases quite rapidly with increasing Hartmann number for the fully developed flow. The Hartmann number is dependent only on the strength of the applied magnetic

field and on the properties of the fluid. Both Stuart and Lock employed an analytical (i.e., asymptotic) method of solution. Their results are, therefore, approximate in nature. To the best knowledge of the author, no numerical solution on the stability of the fully developed Hartmann profiles has been reported.

Recently Chen and Sparrow (4,5) have studied the stability characteristics of developing laminar flow in the entrance region of a parallel-plate channel without the presence of a magnetic field. The stability characteristics they studied correspond to developing profiles induced by a uniform and a linear velocity distribution at the channel inlet. They found that the critical Reynolds number decreases monotonically as the axial distance increases, attaining the limiting value for the fully developed, plane Poiseuille flow. They also found that as the velocity profile becomes more skewed, the flow becomes more stable.

The stability of MHD flow in the entrance region of a parallel-plate channel seems not to have been investigated. Because of the interaction between the changes in the velocity profiles and the induced electromotive force in the entrance region of a MHD channel, it is of interest to study the stability characteristics of such a flow.

C. The Present Investigation

The purpose of this investigation is to examine the coupled problem of the stability of a magnetohydrodynamic flow in the entrance region of a parallel-plate channel. In the present investigation, the linear magnetohydrodynamic stability of flow in the entrance region of a parallel-plate channel under a transverse magnetic field is analyzed. The stability characteristics to be studied here correspond, respectively, to the developing flows induced by a uniform velocity profile (slug flow) and a parabolic velocity profile (hydrodynamically fully developed) at the channel inlet. The stability characteristics of the fully developed Hartmann flow are also re-examined. In the analysis, small, two-dimensional perturbations are superimposed on the main flow. The linearized perturbation equations are then expressed in terms of amplitude functions by introducing stream functions which satisfy the conservation equations. These equations are then reduced into a single magnetohydrodynamic stability equation. The resulting eigenvalue problem is solved by a finite difference scheme similar to that of Chen (6).

Neutral stability curves and critical Reynolds numbers for the Hartmann flow and for the developing flow at various axial locations in the entrance region are obtained. The effect of flow development and the applied

magnetic field on the stability characteristics of flow in the entrance region is studied. The stability results from the present investigation are compared with those reported by Chen and Sparrow (4,5) for the purely hydrodynamic case. In addition, the stability results of the Hartmann flow from the finite difference method of solution will be compared with those of Lock (3) obtained by the asymptotic method of solution.

II. FORMULATION OF THE STABILITY PROBLEM

It has now been well established that the present work deals with the study of the stability of laminar flow of an electrically conducting fluid in the entrance region of a parallel-plate channel under a transverse magnetic field. In the analysis of this problem, it is necessary to first present the governing MHD equations for the main magnetic and flow fields and reduce them to simpler forms by applying the various assumptions of the analysis. These equations are then perturbed with respect to the main fields. After eliminating the main field components, the resulting equations for the disturbances are then simplified to two equations, one for the flow field and the other for the magnetic field. Next, by assuming a small magnetic Reynolds number, these two equations are combined into a single governing differential equation in terms of the amplitude function of the velocity disturbance stream function. This equation together with the appropriate boundary conditions is then converted into finite difference form and solved numerically with the aid of a digital computer. Because the governing stability equation contains terms associated with the velocity component of the main flow and its second

derivative, a brief description of the flow development will be presented prior to the stability analysis.

A. The Governing Equations

Magnetohydrodynamic flows are governed by Maxwell's equations of electromagnetism, Ohm's law of electrical conduction, and, for the present study, the equations of Newtonian fluid motion. For constant fluid properties, these equations in vector form are

Maxwell's Equations

$$\vec{\nabla} \times \vec{H} = \vec{J} \qquad \text{(Ampere's Law)} \quad (1)$$

$$\vec{\nabla} \cdot \vec{B} = 0 \qquad \text{(Magnetic Induction)} \quad (2)$$

$$\vec{\nabla} \times \vec{E} = -\frac{\partial \vec{B}}{\partial t^*} \qquad \text{(Faraday's Law)} \quad (3)$$

$$\vec{\nabla} \cdot \vec{J} = 0 \quad (4)$$

Ohm's Law (without Hall effect)

$$\vec{J} = \sigma(\vec{E} + \vec{V} \times \vec{B}) \quad (5)$$

Continuity Equation

$$\vec{\nabla} \cdot \vec{V} = 0 \quad (6)$$

Equation of Motion (Navier-Stokes Equation)

$$\frac{\partial \vec{V}}{\partial t^*} + (\vec{V} \cdot \vec{\nabla})\vec{V} = \frac{1}{\rho}(\vec{J} \times \vec{B}) - \frac{1}{\rho}\vec{\nabla}p + \nu\nabla^2\vec{V} \quad (7)$$

where all symbols have been defined in the nomenclature.

These governing equations have been established with the application of assumptions commonly employed in the analysis of magnetohydrodynamics. The more significant among these are (a) the electric field force, $\rho_e \vec{E}$, is negligible in comparison with the magnetic force, $\vec{J} \times \vec{B}$, and (b) all velocities are taken to be much less than the speed of light so that no relativistic effects occur. In the present work, the magnetic permeability, μ_m, and the electrical conductivity, σ, of the working fluid are taken as invariant scalar quantities.

One may eliminate the electric field from Equations (5) and (3) and utilize Equation (1) along with the relation $\vec{B} = \mu_m \vec{H}$ to obtain the magnetic transport equation:

$$\frac{\partial \vec{H}}{\partial t^*} = \lambda \nabla^2 \vec{H} + \vec{\nabla} \times (\vec{V} \times \vec{H}), \quad \lambda = \frac{1}{\mu_m \sigma} . \tag{8}$$

By making use of a vector identity and Equations (2) and (6), the magnetic transport equation, Equation (8), can be written as

$$\frac{\partial \vec{H}}{\partial t^*} + (\vec{V} \cdot \vec{\nabla})\vec{H} - (\vec{H} \cdot \vec{\nabla})\vec{V} = \lambda \nabla^2 \vec{H} \tag{9}$$

an equation which proves convenient later in the analysis.

In addition to the assumptions mentioned in writing down the MHD equations, other assumptions of the analysis

will now be discussed. The MHD duct to be considered here is of a parallel-plate channel geometry with the plate width very large in extent in the z* direction. The top and bottom plates are electrically non-conducting. The axial and transverse coordinates, x* and y*, are measured, respectively, from the inlet and centerline of the channel. The height of the channel is 2L so that $-L \leq y^* \leq L$. Since $L << z^*$, the velocity field does not vary in the z* direction. A constant magnetic field of intensity H_o is applied in the y* direction normal to the channel walls. Also, magnetic end effects and MHD end losses are neglected.

The effects of the induced magnetic field, H_x, in the axial direction on the flow field are neglected. In addition, H_x is considered small in comparison with the applied magnetic field, H_o. This implies that the magnetic Reynolds number, R_m, is assumed to be small. The magnetic field in the y* direction, H_y, is assumed constant and equal to H_o. The induced magnetic field, H_x, is considered invariant with respect to x* and z* coordinates. Thus H_x is a function of y* only. The condition that $H_x << H_y = H_o$ can be verified from an order of magnitude analysis as applied to Equation (9) for a steady, two-dimensional magnetic field. The gravitational field force can be neglected in comparison with the

magnetic field force. In addition, Hall currents are assumed absent.

The flow in the entrance region of the channel is assumed to be steady, laminar, and two-dimensional, and the fluid properties are assumed constant. Finally, the Prandtl boundary layer assumptions are assumed valid.

The assumptions that the Prandtl boundary layer assumptions are applicable and that the flow is parallel, i.e., $\bar{u} = \bar{u}(y^*)$, in the entrance region are quite critical to the analysis. Significant uncertainly may be generated at this point because one of the boundary layer assumptions is that in the entrance region the velocity component in the y* direction, $\bar{v}$, is very small compared with the velocity component in the axial direction, $\bar{u}$. Doubts can be raised in neglecting the transverse velocity component, $\bar{v}$, because the fully developed flow (Hartmann profile) occurs in relatively short entrance lengths due to the presence of the relatively large magnetic body force. However, it can be shown from an order of magnitude analysis together with the assumption of small magnetic Reynolds number that the fluid velocity and magnetic field in the axial direction can be considered as functions of y* only, with good accuracy. In his unpublished work, Chen (7) has shown that the parallel flow assumption is quite applicable to the stability

analysis for flows in the entrance region of a parallel channel, providing no mass transfer occurs through the channel walls, either by suction or injection. This conclusion may safely be extended to the stability analysis of MHD channel flows for small Hartmann numbers of, say, less than 10.

B. The Basic Flow

Before proceeding to the execution of the stability analysis, a knowledge of the main flow velocity field in the entrance region of the MHD channel is necessary. The electrically conducting fluid enters the MHD channel with a specified velocity profile, $W_o(y^*)$. The magnetic and viscous forces act on the flow in the channel entrance region until a fully developed, Hartmann profile is established. This Hartmann profile, once established, remains unchanged for the remaining channel length.

The flow development in the entrance region of a MHD channel has been analyzed by many investigators using various approximate methods of solution. Among them are the Karman-Pohlhausen integral method employed by Maciulaitis and Loeffler (8), the patching of the upstream and downstream velocity field technique utilized by Roidt and Cess (9), the finite difference method of solution employed by Hwang, et al. (10,11), and the

application of the linearization method of Sparrow, et. al. (12) by Snyder (13). Very recently Chen (14) employed the linearization technique to obtain solutions for the flow development and pressure drop in the entrance region of a MHD channel for any type of velocity distributions at the channel inlet. These solutions were then specialized for parabolic and linear inlet velocity profiles. The equation Chen solved was a linear form of Equation (7) with the boundary layer assumptions applied.

In the present study, the velocity solutions obtained by Chen (14) will be used in the stability analysis. This work is used because the velocity solutions are expressed as a continuous function of the axial and transverse coordinates all the way from the channel entrance to the fully developed region, so that the velocity and its derivatives can be evaluated with great accuracy. It is well known from the stability analysis that the velocity and its derivatives play an important role in the accuracy of the final results of the stability calculations.

For convenience, highlights of Chen's work (14) will be described briefly. In order to perform his analysis, Chen made the following assumptions: (a) no Hall currents are present, (b) the Prandtl boundary layer equations hold, (c) the pressure is uniform across the channel, (d) the fluid properties are constant, (e) the magnetic

permeability and electrical conductivity are scalar constants, (f) the magnetic end effects and MHD end losses are neglected, and (g) the electric field measured across the channel walls is zero. Therefore, the assumptions made in writing down the governing MHD equations for the problem under consideration are quite compatable with those of Chen.

The linearization technique used by Chen is an extension of the technique developed by Sparrow, et al. (12) for analyzing purely hydrodynamic duct flow problems. His method is to linearize the nonlinear inertia terms in the axial momentum equation by introducing a stretched axial coordinate, $\bar{x}$ or $\bar{X}$, and a function which contains the pressure gradient and the residue of the inertia terms. It is possible to seek a solution of this linearized equation as a linear combination of a fully developed velocity, W_{fd}, and a difference velocity, W^*, which goes to zero as $\bar{X}$ approaches infinity (large axial distances). The details of the solution can be found in the work of Chen (14).

For the case of parabolic inlet velocity profiles, $W_o(y) = 1.5(1 - y^2)$, the velocity solution is given by

$$W(\bar{X},y) = \frac{M(\text{Cosh}M-\text{Cosh}My)}{M\text{Cosh}M-\text{Sinh}M} + \sum_{i=1}^{\infty} \frac{2}{\alpha_i^2} \left(\frac{M^2}{\alpha_i^2+M^2}\right) \cdot \left(1 - \frac{\text{Cos}\alpha_i y}{\text{Cos}\ \alpha_i}\right) \exp[-(\alpha_i^2 + M^2)\bar{X}] \qquad (10)$$

and for the uniform velocity profile at the channel inlet, $W_o = 1$, it is given by

$$W(\bar{X},y) = \frac{M(\text{CoshM}-\text{Cosh}My)}{M\text{Cosh}M-\text{Sinh}M} + \sum_{i=1}^{\infty} \frac{2}{\alpha_i^2+M^2} \left(\frac{\text{Cos}\alpha_i y}{\text{Cos}\ \alpha_i} - 1\right) \cdot \exp[-(\alpha_i^2 + M^2)\bar{X}] \qquad (11)$$

where the α_i are the roots of $\alpha_i = \tan \alpha_i$.

The stretched axial coordinate, $\bar{x}$ (or $\bar{X}$) appearing in Equations (10) and (11) is related to the actual axial coordinate, x* (or X), by the relation

$$x^* = \int_0^{\bar{x}} \varepsilon(M,\bar{x})\, d\bar{x} \quad \text{or} \quad X = \int_0^{\bar{X}} \varepsilon(M,\bar{X})\, d\bar{X} \qquad (12)$$

where

$$\varepsilon(M,\bar{X}) = \frac{\int_0^1 \left(\frac{\partial W}{\partial \bar{X}}\right)\left(2W - \frac{3}{2}W^2\right) dy}{\left(\frac{\partial W}{\partial y}\right)_{y=1} + \int_0^1 \left(\frac{\partial W}{\partial y}\right)^2 dy + M^2 \int_0^1 (W^2-1)\, dy} \qquad (13)$$

The foregoing equations fully specify the magneto-hydrodynamic velocity development expressed as W(=u/U) as a function of X and y for parametric values of Hartmann number, M. The relationship between the actual physical coordinate, X, and the stretched axial coordinate, $\bar{X}$, is

listed in Table B-1, Appendix B. As $\bar{X}$ (or X) approaches infinity, both expressions for W, Equations (10) and (11), reduce to W_{fd}, the fully developed Hartmann profile, given by the first term on the right-hand side of the equations.

For the stability analysis, the second derivatives of the velocity solutions, Equations (10) and (11), with respect to y are needed. For completeness, they are presented here:

For $W_o = 1.5(1 - y^2)$,

$$\frac{\partial^2 W}{\partial y^2} = \frac{-M^3 \text{Cosh} My}{M\text{Cosh}M - \text{Sinh}M} + \sum_{i=1}^{\infty} \frac{2M^2}{\alpha_i^2 + M^2} \frac{\text{Cos}\alpha_i y}{\text{Cos}\ \alpha_i} \cdot \exp[-(\alpha_i^2 + M^2)\bar{X}] \tag{14}$$

For $W_o = 1$,

$$\frac{\partial^2 W}{\partial y^2} = \frac{-M^3 \text{Cosh} My}{M\text{Cosh}M - \text{Sinh}M} - \sum_{i=1}^{\infty} \frac{2\alpha_i^2}{\alpha_i^2 + M^2} \frac{\text{Cos}\alpha_i y}{\text{Cos}\ \alpha_i} \cdot \exp[-(\alpha_i^2 + M^2)\bar{X}] \tag{15}$$

C. The Stability Equation

It is assumed that the main flow, $\bar{u}$, depends on y* only; that is, the flow is parallel. Parallel flow is not exactly the situation encountered in the actual flow under study here. However, in situations in which the flow is nearly unidirectional, it is a standard procedure to

employ the parallel flow model for the purpose of the stability analysis. The flow in the entrance region of a magnetohydrodynamic channel is nearly parallel.

By employing the parallel flow model and an order of magnitude comparison together with the approximation of small magnetic Reynolds number, the various vector quantities representing the basic flow and magnetic fields associated with the MHD equations for a steady, two-dimensional channel problem are

$$\vec{V} = (\bar{u},0) \tag{16}$$

$$\vec{H} = (H_x,H_y);\ H_y = H_o,\ \text{a constant} \tag{17}$$

$$\vec{J} = \vec{\nabla} \times \vec{H} = \left(\frac{\partial H_y}{\partial x^*} - \frac{\partial H_x}{\partial y^*}\right)\hat{k} \tag{18}$$

The continuity equation, the Navier-Stokes equation of Newtonian fluid motion, and the magnetic transport equation, given in vector form in Equations (6), (7), and (9), respectively, may be written in component form for a two-dimensional problem as

$$\frac{\partial u}{\partial x^*} + \frac{\partial v}{\partial y^*} = 0 \tag{19}$$

$$\frac{\partial u}{\partial t^*} + u\frac{\partial u}{\partial x^*} + v\frac{\partial u}{\partial y^*} = \frac{\mu_m}{\rho} H_y \left(\frac{\partial H_x}{\partial y^*} - \frac{\partial H_y}{\partial x^*}\right) - \frac{1}{\rho}\frac{\partial p}{\partial x^*} + \nu\left(\frac{\partial^2 u}{\partial x^{*2}} + \frac{\partial^2 u}{\partial y^{*2}}\right) \tag{20}$$

$$\frac{\partial v}{\partial t^*} + u\frac{\partial v}{\partial x^*} + v\frac{\partial v}{\partial y^*} = \frac{\mu_m H_x}{\rho}\left(\frac{\partial H_y}{\partial x^*} - \frac{\partial H_x}{\partial y^*}\right) - \frac{1}{\rho}\frac{\partial p}{\partial y^*} + \nu\left(\frac{\partial^2 v}{\partial x^{*2}} + \frac{\partial^2 v}{\partial y^{*2}}\right) \tag{21}$$

$$\frac{\partial H_x}{\partial t^*} + u\frac{\partial H_x}{\partial x^*} + v\frac{\partial H_x}{\partial y^*} - H_x\frac{\partial u}{\partial x^*} - H_y\frac{\partial u}{\partial y^*} = \frac{1}{\sigma\mu_m}\left(\frac{\partial^2 H_x}{\partial x^{*2}} + \frac{\partial^2 H_x}{\partial y^{*2}}\right) \tag{22}$$

$$\frac{\partial H_y}{\partial t^*} + u\frac{\partial H_y}{\partial x^*} + v\frac{\partial H_y}{\partial y^*} - H_x\frac{\partial v}{\partial x^*} - H_y\frac{\partial v}{\partial y^*} = \frac{1}{\sigma\mu_m}\left(\frac{\partial^2 H_y}{\partial x^{*2}} + \frac{\partial^2 H_y}{\partial y^{*2}}\right) \tag{23}$$

It has been shown by Stuart (2), Lock (3), and others that Squire's theorem (15) applies as well in deriving the stability equation for MHD channel flow, provided that the magnetic Reynolds number is small. This is quite significant because this means that, for flow in a channel, the main flow is less stable to two-dimensional disturbances than to the three-dimensional disturbances. It, therefore, suffices to consider only the two-dimensional disturbances in the present stability analysis.

The derivation of the stability equation is detailed in Appendix A. It suffices to show only the highlights of the derivation here.

Following Lock (3), the two-dimensional system, Equations (19) through (23), is perturbed with respect to two-dimensional disturbances and linearized. The resultant quantities are composed of a main flow expression plus a perturbation expression, see Equation (A-3). Stream function solutions of the velocity and magnetic field components, Equation (A-9), are then substituted into the perturbation equation of motion, Equations (A-4) and (A-5). Cross-differentiation of the perturbation equations of motion eliminates the pressure gradient terms. After rearranging terms and introducing dimensionless variables, Equation (A-11), one arrives at

$$(W - c)(\phi'' - \alpha^2\phi) - W''\phi = \frac{1}{i\alpha R}(\phi^{iv} - 2\alpha^2\phi'' + \alpha^4\phi) + \frac{M^2}{RR_m}[h(\theta'' - \alpha^2\theta) - \theta h'' + \frac{i}{\alpha}(\alpha^2\theta' - \theta''')] \tag{24}$$

Applying the assumption of small magnetic Reynolds number to the x-component of the magnetic transport equation, one finds, after taking the derivative with respect to y of the reduced x-magnetic transport equation,

$$(\theta''' - \alpha^2\theta') \simeq -R_m\phi'' \tag{25}$$

Applying the assumption of small magnetic Reynolds number (h is very small) and incorporating Equation (25) into Equation (24), one obtains

$$(W - c)(\phi'' - \alpha^2\phi) - W''\phi = \frac{1}{i\alpha R}(\phi^{iv} - 2\alpha^2\phi'' + \alpha^4\phi) - \frac{M^2\phi''}{i\alpha R} \tag{26}$$

where W and c ($=c_r + c_i$) are, respectively, the main flow velocity and the complex wave velocity normalized by the average velocity, U; α is the wave number based on L; $R(=LU/\nu)$ is the Reynolds number; $M(=\mu_m H_o L(\sigma/u_f)^{1/2})$ is the Hartmann number. The primes denote derivatives with respect to y.

The disturbance amplitude function for the velocity field, ϕ, is related to the fluid stream function, Ψ, by the expression

$$\Psi(x,y,t) = \phi(y)\ \exp[i\alpha(x-ct)] \tag{27}$$

If c_i is negative, the disturbances decay and the flow is stable. On the other hand, if c_i is positive, the disturbances are amplified and the flow is unstable. The condition of neutral stability is characterized by $c_i = 0$. The stream function, Ψ, is satisfied by the continuity equation. It is to be noted that Equation (26) reduces to the conventional Orr-Sommerfeld equation when M = 0. Equation (26) is the governing equation for the magnetohydrodynamic stability problem under consideration, expressed in terms of the disturbance amplitude function of the velocity field.

D. The Boundary Conditions

Equation (26) is a fourth order differential equation in ϕ and may be solved subject to four boundary conditions. The boundary conditions for ϕ which arise from zero disturbance velocity at the channel walls, namely $u^*=v^*=0$ at $y = \pm L$ are

$$\phi(1) = \phi'(1) = 0 \tag{28a}$$

$$\phi(-1) = \phi'(-1) = 0 \tag{28b}$$

In the present investigation, only velocity profiles which are symmetric with respect to the centerline of the channel are considered. To expediate computations, it is therefore advantageous to consider only half of the channel in the stability analysis. Since the basic flow is an even function of y, the solution for $\phi(y)$ can be decomposed into even and odd modes. Of primary importance, however, is the case of even ϕ; because, the work of Grohne (16) has strongly suggested that, for plane Poiseuille flow, only this mode is likely to lead to instability of the flow. Thus, the boundary conditions corresponding to the bottom wall, Equation (28b), can be replaced by those at the center of the channel. For ϕ even, they are

$$\phi'(0) = \phi'''(0) = 0 \tag{28c}$$

The mathematical system consisting of Equations (26), (28a), and (28b) (or (28c)) constitutes an eigenvalue

problem. In the present analysis, this system was solved by a finite difference scheme which is described in the following section.

III. THE FINITE DIFFERENCE METHOD OF SOLUTION

A. Formulation of the Finite Difference Equations

The formulation of the finite difference equations presented here follows closely the work of Chen (6) in his analysis of the hydrodynamic stability of flow in the entrance region of a parallel-plate channel. Equation (26) can be expressed as a linear algebraic equation of the form

$$\mathcal{L}\phi = c\mathcal{M}\phi \tag{29}$$

where $\mathcal{L}$ and $\mathcal{M}$ are linear operators defined as

$$\mathcal{L} = W(D^2 - \alpha^2) - W'' + \frac{i}{\alpha R}\left[D^4 - (M^2+2\alpha^2)D^2 + \alpha^4\right] \tag{30}$$

and

$$\mathcal{M} = (D^2 - \alpha^2) \tag{31}$$

In these equations, D^n represents d^n/dy^n.

The well known transformation matrix in finite difference form for a function g and its derivatives accurate to the order of the mesh size squared, r^2, is

$$\begin{bmatrix} g \\ rDg \\ r^2D^2g \\ r^3D^3g \\ r^4D^4g \end{bmatrix} = \begin{bmatrix} 1 & 0 & 0 & 0 & 0 \\ 0 & 1 & 0 & 0 & 0 \\ 0 & 0 & 1 & 0 & 0 \\ 0 & 0 & 0 & 1 & 0 \\ 0 & 0 & 0 & 0 & 1 \end{bmatrix} \begin{bmatrix} g \\ \mu\delta g \\ \delta^2 g \\ \mu\delta^3 g \\ \delta^4 g \end{bmatrix} + \begin{bmatrix} 0 \\ 0(r^3) \\ 0(r^4) \\ 0(r^5) \\ 0(r^6) \end{bmatrix} \tag{32}$$

where

$$\begin{bmatrix} g \\ \mu\delta g \\ \delta^2 g \\ \mu\delta^3 g \\ \delta^4 g \end{bmatrix} = \begin{bmatrix} 0 & 0 & 1 & 0 & 0 \\ 0 & -1/2 & 0 & 1/2 & 0 \\ 0 & 1 & -2 & 1 & 0 \\ -1/2 & 1 & 0 & -1 & 1/2 \\ 1 & -4 & 6 & -4 & 1 \end{bmatrix} \begin{bmatrix} g(y-2r) \\ g(y-r) \\ g(y) \\ g(y+r) \\ g(y+2r) \end{bmatrix} \tag{33}$$

In Equations (32) and (33), δ and μ are, respectively, the central difference operator, and the averaging operator. The column vector of error magnitudes has been added to the transformed matrix, Equation (32), to show the truncation error. It can be seen that g and its derivatives at a point y are now represented in finite difference form by five equally spaced, discrete points a distance r apart. To reduce the truncation error, Thomas (17) introduced the transformation

$$g(y) = (1 - \frac{1}{6}r^2D^2 + \frac{1}{90}r^4D^4)\phi(y) \tag{34}$$

With this transformation of the variable $\phi(y)$, it can be shown from finite differences that

$$\begin{bmatrix} \phi \\ rD\phi \\ r^2D^2\phi \\ r^3D^3\phi \\ r^4D^4\phi \end{bmatrix} = \begin{bmatrix} 1 & 0 & 1/6 & 0 & 1/360 \\ 0 & 1 & 0 & 0 & 0 \\ 0 & 0 & 1 & 0 & 1/12 \\ 0 & 0 & 0 & 1 & 0 \\ 0 & 0 & 0 & 0 & 1 \end{bmatrix} \begin{bmatrix} g \\ \mu\delta g \\ \delta^2 g \\ \mu\delta^3 g \\ \delta^4 g \end{bmatrix} + \begin{bmatrix} 0(r^8) \\ 0(r^5) \\ 0(r^8) \\ 0(r^5) \\ 0(r^8) \end{bmatrix} \tag{35}$$

Substituting Equation (33) into Equation (35) one arrives at

$$\begin{bmatrix} \phi \\ rD\phi \\ r^2D^2\phi \\ r^3D^3\phi \\ r^4D^4\phi \end{bmatrix} = \begin{bmatrix} 1/360 & 7/45 & 41/60 & 7/45 & 1/360 \\ 0 & -1/2 & 0 & 1/2 & 0 \\ 1/12 & 2/3 & -3/2 & 2/3 & 1/12 \\ -1/2 & 1 & 0 & -1 & 1/2 \\ 1 & -4 & 6 & -4 & 1 \end{bmatrix} \begin{bmatrix} g(y-2r) \\ g(y-r) \\ g(y) \\ g(y+r) \\ g(y+2r) \end{bmatrix} + \begin{bmatrix} 0(r^8) \\ 0(r^5) \\ 0(r^8) \\ 0(r^5) \\ 0(r^8) \end{bmatrix} \tag{36}$$

Thus, a fourth order differential equation of ϕ may be approximated by a finite difference equation in g which is accurate to the order r^4, providing that no third derivatives appear. It is clear that ϕ and its derivatives at a point are now related to g at five equally spaced, discrete points. This work obviously permits the MHD stability equation to be expressed as a finite difference equation accurate to r^4. For r equal to, say, 0.01, the finite difference approximation of the differential equation introduces a discretization error of 10^{-8}.

In the numerical calculations, the channel half-height ($0 \leq y \leq 1$) was subdivided into N equal intervals or steps and the finite difference equations applied to (N+1) points in the finite difference mesh, thereby generating (N+1) simultaneous, homogeneous, algebraic equations.

To formulate the system of algebraic equations, Equation (29) is expressed in matrix form as

$$[A][g] = c[B][g] \tag{37}$$

where

$$[B] \cong \mathcal{M} = (D^2 - \alpha^2) \text{ and}$$

$$[A] \cong \mathcal{L} = W(D^2 - \alpha^2) - W'' + \frac{i}{\alpha R}[D^4 - (M^2 + 2\alpha^2) + \alpha^4]$$

show the finite difference approximations to the differential operators. [A] and [B] are (N+1) X (N+1) coefficient matrices, [g] is the vector representing the discrete functional values after the transformation, Equation (34), and c is the complex valued velocity of wave propagation.

Using the transformation matrix, Equation (36), it may be readily shown that

$$[B][g] = \bar{a}_1 \cdot g(y-2r) + \bar{a}_2 \cdot g(y-r) + \bar{a}_3 \cdot g(y) + \bar{a}_2 \cdot g(y+r) + \bar{a}_1 \cdot g(y+2r) \tag{38}$$

where

$$\bar{a}_1 = \frac{1}{r^2}\left(\frac{1}{12} - \frac{1}{360} r^2\alpha^2\right)$$

$$\bar{a}_2 = \frac{1}{r^2}\left(\frac{2}{3} - \frac{7}{45} r^2\alpha^2\right) \tag{39}$$

$$\bar{a}_3 = \frac{1}{r^2}\left(-\frac{3}{2} - \frac{41}{60} r^2\alpha^2\right)$$

Similarly,

$$[A][g] = (a_1+ib_1)\cdot g(y-2r)+(a_2+ib_2)\cdot g(y-r)$$
$$+ (a_3+ib_3)\cdot g(y)+(a_2+ib_2)\cdot g(y+r) \qquad (40)$$
$$+ (a_1+ib_1)\cdot g(y+2r)$$

In Equation (40), the a's are given by

$$a_1 = (W\bar{a}_1 - \frac{W''}{360})$$
$$a_2 = (W\bar{a}_2 - \frac{7}{45}W'') \qquad (41)$$
$$a_3 = (W\bar{a}_3 - \frac{41}{60}W'')$$

and the b's are given by

$$b_1 = \frac{1}{r^2\alpha R}\left[\frac{1}{r^2} - \frac{1}{12}(M^2 + 2\alpha^2) + \frac{1}{360} r^2\alpha^4\right]$$
$$b_2 = \frac{1}{r^2\alpha R}\left[-\frac{4}{r^2} - \frac{2}{3}(M^2+2\alpha^2) + \frac{7}{45} r^2\alpha^4\right] \qquad (42)$$
$$b_3 = \frac{1}{r^2\alpha R}\left[\frac{6}{r^2} + \frac{3}{2}(M^2 + 2\alpha^2) + \frac{41}{60} r^2\alpha^4\right]$$

The independent variable, y, takes on the discrete values $0, r, 2r, \ldots, (N-1)\cdot r$, $Nr = 1$ for the symmetric profiles considered in this investigation.

In order to evaluate the quantities on the right-hand sides of Equations (38) and (40) at the boundaries y=0 (channel centerline) and y=1 (upper wall), one needs to

know the values of g at two points which are outside of each of the boundaries. These values are obtained by applying the boundary conditions in conjunction with Equation (36). Application of Equation (28a) gives

$$g((N+1)\cdot r) = g((N-1)\cdot r) \tag{43}$$

$$g((N+2)\cdot r) = -g((N-2)\cdot r) - 112g((N-1)\cdot r) - 246g(N\cdot r)$$

The boundary conditions at the center of the channel are given by Equation (28c). These result in

$$\begin{aligned} g(-r) &= g(r) \\ g(-2r) &= g(2r) \end{aligned} \tag{44}$$

Equations (38), (40), (43), and (44) provide complete information for writing (N+1) simultaneous, complex, algebraic equations given by the relation

$$[A][g] - c[B][g] = 0 \tag{45a}$$

or

$$[D(\alpha,c,R,M)][g] = 0 \tag{45b}$$

Since these equations are linear and homogeneous, it is necessary that the determinant of the coefficient matrix must be zero in order that a solution exists, that is,

$$\text{Det}|[D(\alpha,c,R,M)]| = 0 \tag{46}$$

When the elements of the coefficient matrix [D] are written out, it can be seen that there are five non-zero elements clustered in the vicinity of the main diagonal; that is, the matrix [D] is of a stripe nature.

B. The Eigenvalue Problem

In the preceding section, the eigenvalue problem consisting of Equations (26), (28a), and (28c) was converted into a secular equation given by Equation (46). The eigenvalue problem consists of finding the values of c which satisfy Equation (46) for given values of α, M, and R. The c value is found by employing an iterative root-finder technique first devised by Muller (18).

The root-finder technique involves the evaluation of the determinant of the coefficient matrix [D] at three points in the complex c-plane. A complex parabola is fitted through these three points and then extrapolated to zero; this process being repeated iteratively using the three previous points until the criteria for convergence of c are satisfied. The iteration was terminated when both the deviation of the real and imaginary parts of c from two successive iterations became smaller than a preassigned tolerance of 1×10^{-5}. To initiate the iteration, one needs three values of c. With one value of c assigned, the others were chosen to be 1.04c and 0.96c.

It must be pointed out that the number of eigenvalues satisfying Equation (45b) for given M,α, and R are equal to the size of the matrix; thus, there are (N+1) eigenvalues when the region of interest is subdivided into N intervals with (N+1) mesh points. Of primary interest in the stability analysis is the eigenvalue which gives the least stable mode of the flow to the small disturbances; that is, the eigenvalue, c, with the largest value in its imaginary part. The determination of the least stable eigenvalue corresponding to a set of (α,R,M) is very important. In the present study, the least stable eigenvalues for the fully developed Hartmann flow for different Hartmann numbers were determined by using the known value of c for a given α,R, and M from plane Poiseuille flow (M = 0) as the initial guess or assigned value, M being increased from 0 to 1,2,3,4, and so on, while α, R were kept unchanged. Once the least stable eigenvalues for the fully developed Hartmann flow were available, they were used as the initial guess values to find the eigenvalues in the entrance by decreasing $\bar{X}$, the stretched axial coordinate. One thus may proceed anywhere in the (α,R,M,$\bar{X}$) space by utilizing a known least stable eigenvalue, c, and varying <u>one</u> of the four parameters in such a manner that the iterative root-finding technique will again converge to the least stable eigenvalue for the new set of (α,R,M,$\bar{X}$).

C. The Effect of Step Size on Eigenvalues

In the numerical solution of the MHD stability problem, the accuracy of the results are strongly dependent on the finite difference mesh or step spacing, r=1/N; this phenomenon is inherent to all finite difference solutions. This section describes and illustrates how the step size is determined for use in obtaining the results such that a high degree of accuracy in the results is assured.

For the finite difference scheme of this investigation, as the finite difference step size decreases, the finite difference solution approaches the exact solution. Further, because the discretization error of the present finite difference solution is of the order of r^4, the exact solution is approached quite rapidly as r is decreased (i.e., N is increased). Since in this work the stability results are centered around neutral stability ($c_i = 0$), the response of c_i to changes in step size is the criterion used to determine the proper step size. However, it is to be noted that computational time necessarily increases rapidly with the accuracy of the solution. Thus, in the selection of step size, there are two diametrically opposed factors - economics versus accuracy.

The velocity profile dictates the step size necessary for the desired accuracy. For fully developed or Hartmann flow, only the Hartmann number influences the velocity

profile and thus the step size. For developing flow in the duct entrance region, three parameters influence the step size selection:

(a) W_o, the entering velocity profile - particularly dominating near the entrance,

(b) M, the Hartmann number - particularly dominating at large axial distances, and

(c) X or $\bar{X}$, the channel position - an indicator of which of (a) and (b) is more significant.

In the fully developed region it is sufficient to fix α, R, and M and vary N until the exact solution is approached, i.e., until c_i becomes relatively unchanged with increase in N. In this manner, one may determine a proper step size for large axial distances for a given Hartmann number. Table 1 gives the step size determination technique for M = 10 and M = 6. For M = 10 it is found that 300 steps are necessary for sufficient accuracy while 250 are sufficient for M = 6. Table 2 illustrates the effect of step size on the critical Reynolds number for the fully developed flow for Hartmann numbers of 3,4,6, and 10. Results from an insufficient value of N are presented to compare with those of the selected value of N. Note that there is a pronounced effect of the step size on

Table 1

The Effect of Step Size on Eigenvalues for the Fully Developed Hartmann Flow, M = 10 and 6

M = 10		M = 6	
N	c_i	N	c_i
100	-0.1535D-06*	175	0.8537D-06
125	-0.3064D-02	200	0.1290D-03
150	-0.2688D-02	225	0.1981D-03
175	-0.2238D-03	250	0.2379D-03
200	0.1417D-02	275	0.2619D-03
225	0.2225D-02		
250	0.2766D-02		
275	0.3130D-02		
300	0.3379D-02		
⋮			
375	0.3760D-02		

* D-xx = 10^{-xx}

Table 2

The Effect of Step Size on Critical Reynolds Numbers for the Fully Developed Hartmann Flow

M	N	R_{crit}	N*	R_{crit}
3	100	49755	150	48630
4	100	95960	150	89000
6	175	191600	250	184600
10	100	1117000	300	415200

*Step size assuring accurate results

the critical Reynolds number for the case of M = 10. For M less than 3, it can be seen that N = 100 is sufficient to give accurate numerical results.

In the entrance region of the MHD channel, the entering flow, W_o, dictates the necessary step size for a given M and $\bar{X}$ ($\bar{X}$ is now a parameter in the velocity profile). The necessary step size approaches that of the fully developed flow as $\bar{X}$ increases. It is known from the work of Chen and Sparrow (4,5) that 100 steps are sufficient to obtain accurate results for the plane Poiseuille flow profile, while a very large number of steps (or very small step sizes) are necessary for flow in the region very near the entrance of the channel (due to the thin boundary layer) for the case of uniform inlet profile. To assure accuracy of results, it is necessary that the step size be decreased (or the number of steps increased) in the axial direction for the case of parabolic inlet velocity profile. For the case of uniform inlet velocity profile, the step size may be increased in the axial direction as the flow approaches the fully developed Hartmann profile. Table 3 illustrates the effect of step size on the eigenvalues at various axial locations for the case of linear inlet velocity profile when M = 4. Note that the value of N = 200 can be used from near the fully developed region (X = 0.1) up to a location of X = 0.03 in the entrance region with sufficient numerical accuracy.

Table 3

The Effect of Step Size on Eigenvalues for M = 4, Uniform Inlet Velocity Profile

	N = 100	N = 150	N = 200	N = 250
X	c_i	c_i	c_i	c_i
0.100	-0.4091D-03	0.8435D-04	0.1702D-03	0.1937D-03
0.080	-0.3200D-03	0.1757D-03	0.2620D-03	0.2856D-03
0.060	-0.1341D-03	0.3669D-03	0.4541D-03	0.4780D-03
0.050	0.2325D-04	0.5290D-03	0.6171D-03	0.6412D-03
0.040	0.2412D-03	0.7550D-03	0.8400D-03	0.8690D-03
0.030	0.5037D-03	0.1032D-02	0.1124D-02	0.1149D-02
0.020	0.5709D-03	0.1127D-02	- -	0.1251D-02
0.010	-0.1865D-02	0.1235D-02	- -	-0.109 D-02
0.005	-0.8730D-02	- -	- -	-0.786 D-02

For the case of parabolic inlet velocity profile, N = 100 was found to be sufficient for the entire flow region when M is less than 3, while for M = 4 and 6, the number of steps, N, had to be increased from 100 at the inlet to, respectively, 150 and 250 as the flow became fully developed. Table 4 gives the number of steps, N, used in the final stability calculations for parabolic and uniform inlet velocity profiles for all Hartmann numbers and channel positions considered.

D. Method of Generating the Neutral Stability Curves

In the study of hydrodynamic and magnetohydrodynamic stability of flows, the primary interest is to find the neutral stability curve (i.e., the curve $c_i = 0$ which separates the region of stability from that of instability in the wave number versus Reynolds number plane) and the critical Reynolds number (i.e., the minimum Reynolds number possible for the onset of theoretical instability). To generate the neutral stability curves for flow in the fully developed region and developing flow in the entrance region of the MHD channel, the following computational procedure was employed. Depending on the behavior of the neutral stability curve, either α was fixed and R varied or R was fixed and α varied and the corresponding eigenvalues found from Equation (46). With three or more R,

Table 4

Selected Step Sizes Used in the Stability Calculations

Parabolic Inlet Velocity Profile						Uniform Inlet Velocity Profile			
X	M = 1	2	3	4	6	M = 1	2	3	5
∞	100	100	150	150	250	100	100	150	150
0.100	100	100	125	125	-	100	-	125	200
0.080	-	-	125	125	-	100	100	125	-
0.060	100	100	125	125	175	100	-	-	200
0.050	-	-	-	-	-	100	100	125	-
0.040	100	-	125	125	175	125	-	-	200
0.030	-	100	-	-	-	125	125	125	-
0.020	100	-	125	125	175	125	125	150	250
0.010	100	100	100	100	-	125	125	160	250
0.007	-	-	-	-	-	-	125	-	250
0.005	100	100	100	100	-	150	225	225	250
0.003	-	-	-	100	-	200	250	-	275
0.002	100	100	100	100	-	-	-	275	300
0.001	-	-	-	100	-	-	-	-	300

c_i (or α, c_i) pairs available, Aitken's method of interpolation was used to determine the α(or R) value corresponding to $c_i = 0$. This approach facilitated the mapping of the neutral stability curve (locus of α versus R for $c_i = 0$).

Neutral stability curves, critical Reynolds numbers, and other stability characteristics for the two types of developing flows, namely, those induced by parabolic and uniform inlet velocity profiles, were obtained for various Hartmann numbers. All computations were performed with double precision (sixteen decimal) arithematic on an IBM 360/50 digital computer. The stability characteristics of the flow will be presented in the next chapter.

IV. THE NEUTRAL STABILITY RESULTS

In this chapter, representative neutral stability results are presented for the fully developed Hartmann flow and the developing flows. These include neutral stability curves and axial variation of the critical Reynolds number for several Hartmann numbers. The various tables corresponding to the results discussed in this section are given in Appendix B.

A. Fully Developed Hartmann Flow

In Figure 1 are given neutral stability curves for fully developed Hartmann flow for Hartmann numbers of 0, 1, 2, 3, and 4. The wave number, α, is based on the half-height of the channel, L, and the Reynolds number on the average velocity U. These results are tabulated in Table B-2, Appendix B. Also included in the table is the dimensionless velocity of wave propagation, c_r. The curve for M = 0 represents the hydrodynamically fully developed flow (i.e., plane Poiseuille flow), $W = 1.5(1-y^2)$, and is taken from Chen (7). The broken lines are the results of Lock (3) and are presented for comparison. It should be noted that Lock solved analytically the following reduced form of Equation (26) in his investigation:

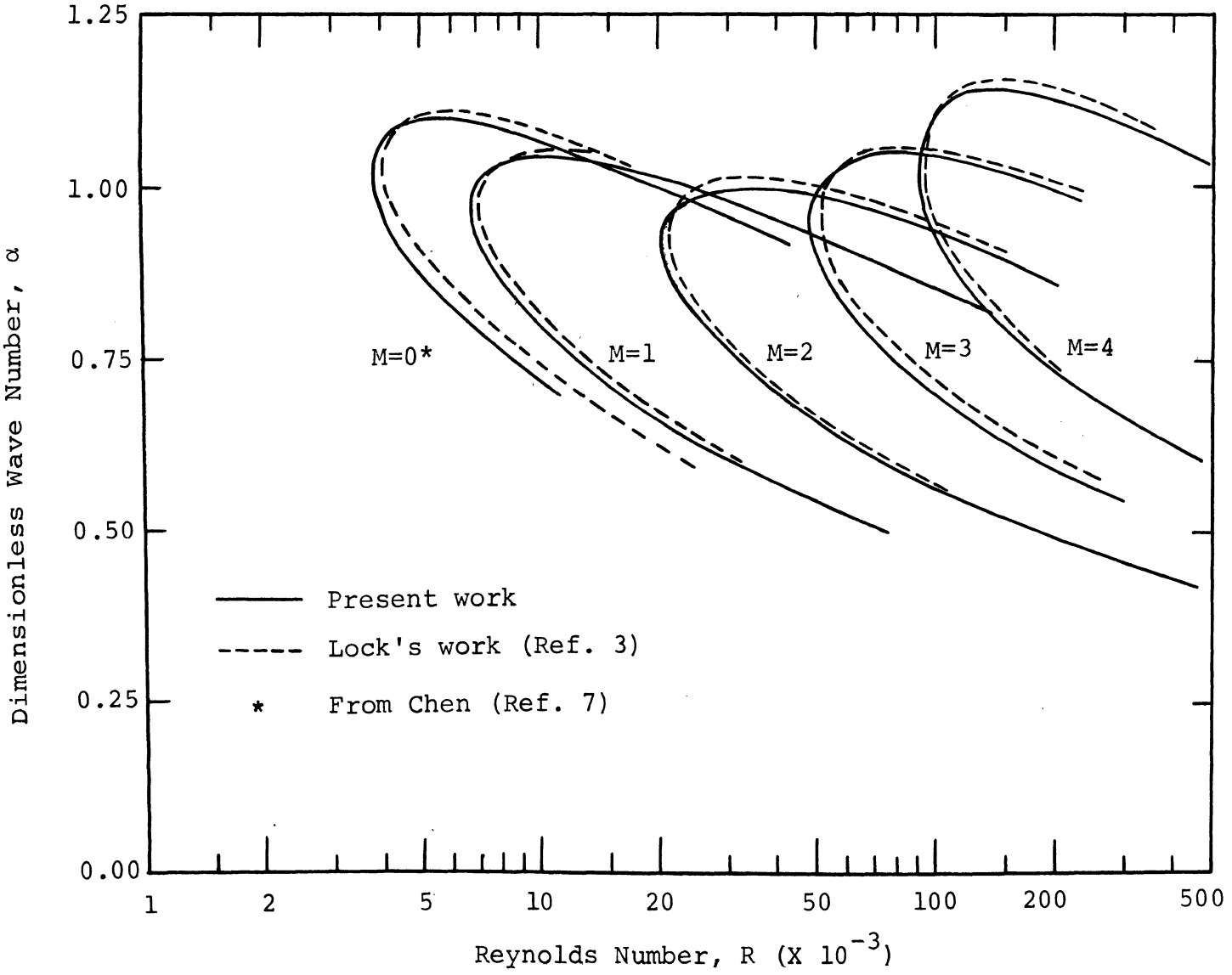

Figure 1: Neutral Stability Curves for Fully Developed Hartmann Flow

$$(W-c)(\phi'' - \alpha^2\phi) - W''\phi = \frac{-i}{\alpha R}\phi^{iv} \qquad (47)$$

It is seen for Figure 1 that the analytical (asymptotic) solution gives neutral stability curves which lie slightly to the right of those obtained from the finite difference method of solution; that is, it predicts critical Reynolds numbers which are higher for all Hartmann numbers examined. Nevertheless, the numerically determined stability results are very nearly the same as those from the analytical solution. The neutral stability results for the critical condition from the present work and the work of Lock are compared in Table B-3 for Hartmann numbers of 0,1,2,3,4,6, and 10.

An inspection of Table B-3 reveals that the critical Reynolds number increases rapidly with increase in the Hartmann number. This conclusion, first established by Lock (3), is due to the effect of the magnetic field on the fully developed velocity profile in a parallel-plate channel.

It is known from early investigations in hydrodynamic stability that the shape of the velocity profile has a pronounced effect on the stability results. Specifically, the flatter the velocity profile away from the wall and the steeper the velocity gradient near the wall (i.e., $\partial W/\partial y$ at $y = \pm 1$), the more stable is the flow (see also Schlichting

(1)). To illustrate this, one can note the following two extreme cases. A laminar flow with uniform velocity profile is known to be absolutely stable, i.e., $R_{crit} = \infty$. This velocity profile is perfectly flat, and the velocity derivative with respect to y, W', at the upper wall is $-\infty$. On the other hand, for the fully developed hydrodynamic flow in a parallel-plate channel (i.e., plane Poiseuille flow), the velocity profile is not flat and the derivative of the velocity with respect to y is -3.0 at the upper wall. It is known that this flow has a critical Reynolds number of 3850 (based on average velocity).

For the fully developed Hartmann profiles, increase in the Hartmann number enhances the flattening of the velocity profile around the center of the channel and increases the magnitude of the velocity gradient at the walls. This behavior of the velocity profile with respect to changes in Hartmann number qualitatively explains the increase in the stability of MHD flows with increase in the Hartmann number.

B. Developing Flow - Parabolic Inlet Velocity Profile

In the previous section, it was mentioned that the plane Poiseuille flow has a known critical Reynolds number of 3850. The critical Reynolds numbers for the fully developed Hartmann flow are also known and have a much

higher value, depending on the Hartmann number. How the overall stability characteristics vary as the flow develops from the plane Poiseuille profile at the channel entrance to the Hartmann profile is one of the primary objectives of this investigation.

Figure 2 has been prepared to show the effect of channel position and Hartmann number (magnetic field strength) on the neutral stability curves for the developing flow with parabolic inlet velocity profile. Because of the rather lengthy computations, only the curves for $M = 1, 3$ and $X = 0.005, 0.020$, and ∞ are given. The stability characteristics corresponding to Figure 2 are listed in Table B-4. Figure 3 shows the variation of the critical Reynolds number with channel position. The data for the curves in Figure 3 are tabulated in Table B-5, Appendix B.

For $M = 0$, the critical Reynolds number remains constant since the inlet velocity profile is the fully developed profile and thus does not change with axial position. For small Hartmann numbers, say, less than 2, the critical Reynolds numbers for the fully developed Hartmann flow are approached very smoothly with a very small or no "over-shoot" which decays monotonically with increasing axial position. For larger Hartmann numbers ($M > 2$), the flow stability tends to increase very rapidly

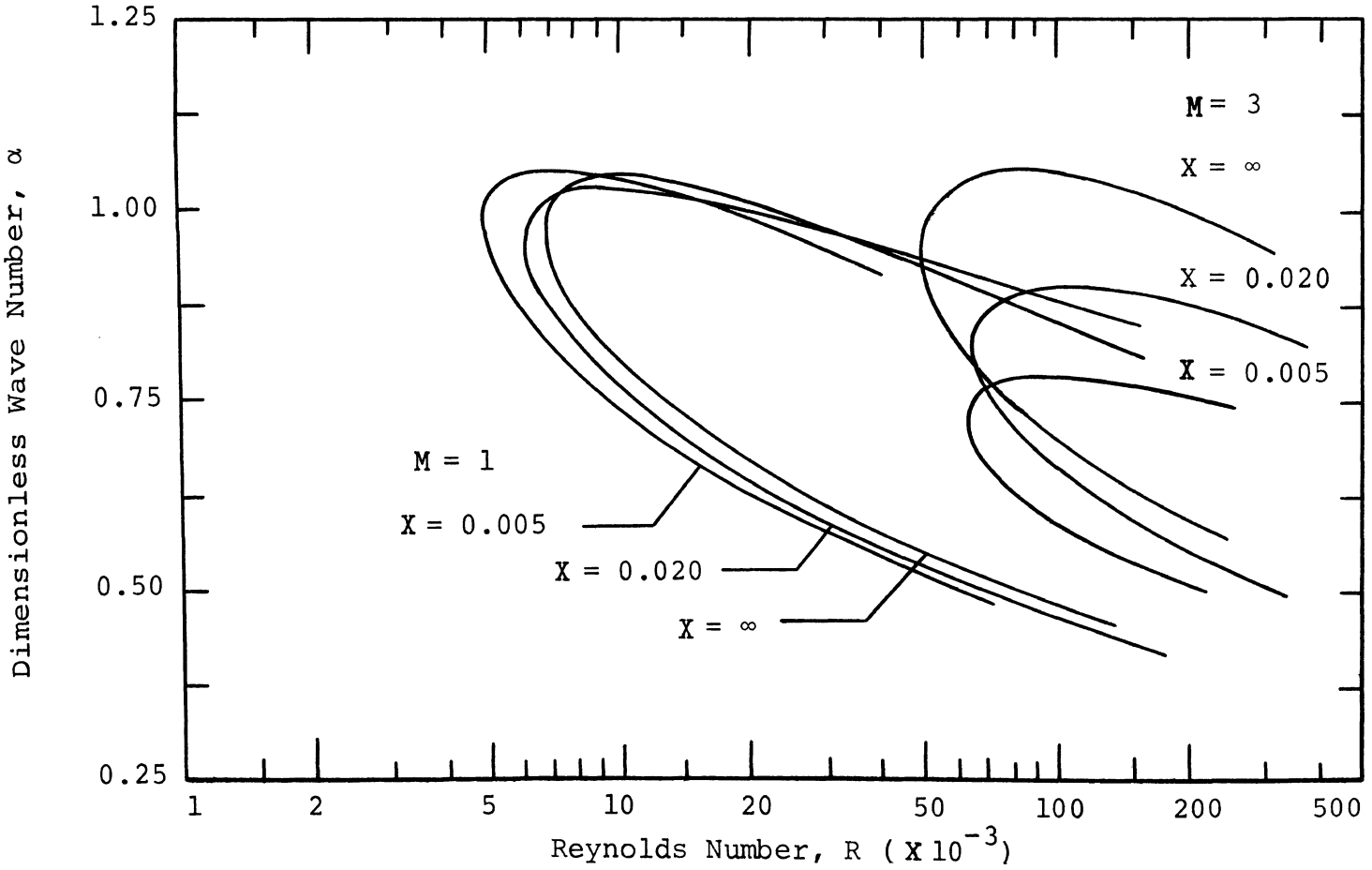

Figure 2: Representative Neutral Stability Curves for the Developing Flow, Parabolic Inlet Velocity Profile

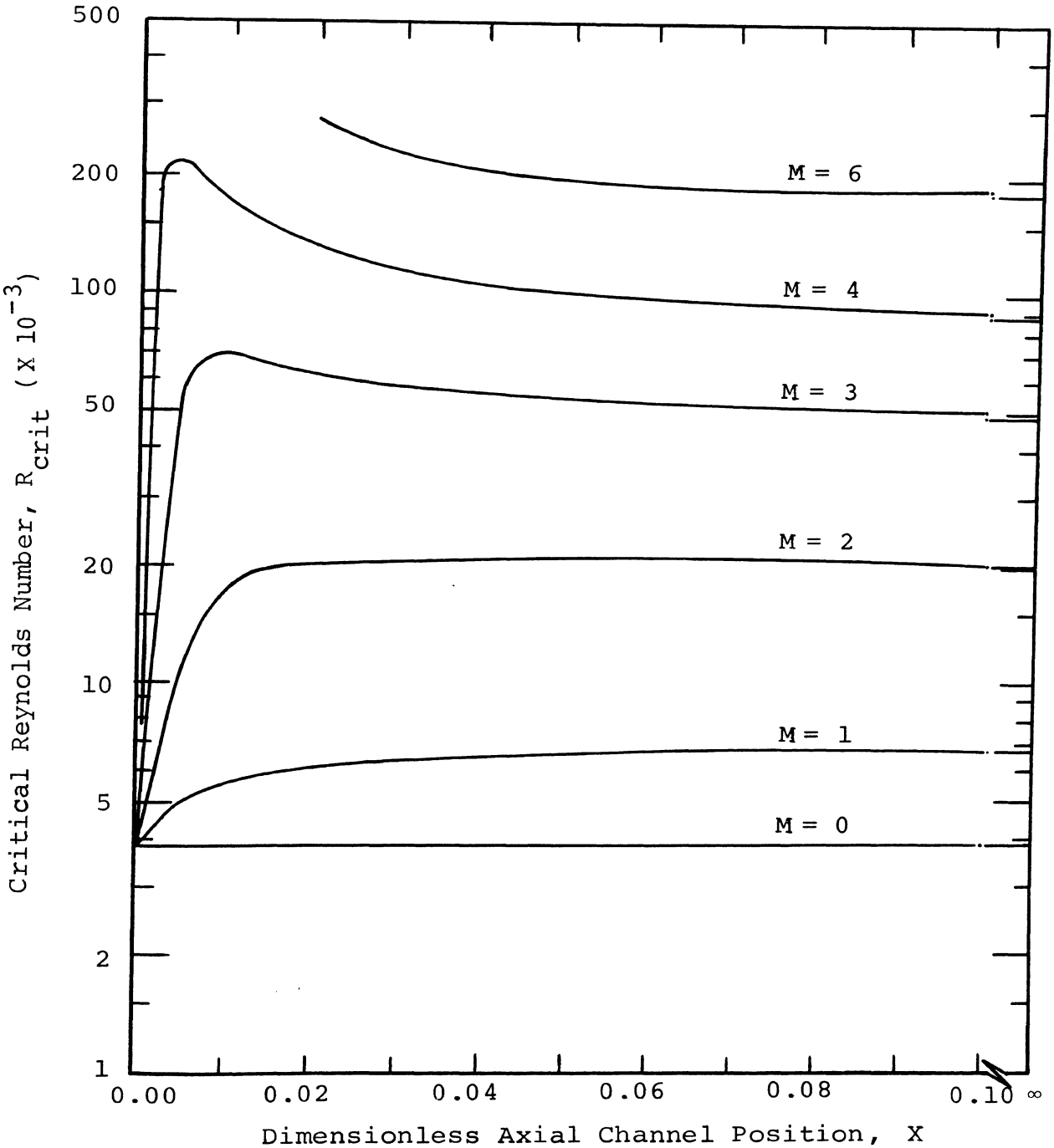

Figure 3 : Variation of the Critical Reynolds Number with Axial Position, Parabolic Inlet Velocity Profile

in the near inlet region and greatly over-shoots the fully developed, critical Reynolds number and approaches this value monotonically from above as the axial distance increases further. As is expected, near the entrance, the critical Reynolds number approaches 3850 as X approaches zero. The behavior of the critical wave number, α_{crit}, as the flow developes under the influence of the parabolic inlet velocity profile is the opposite of that of the critical Reynolds number; that is α_{crit} first decreases from 1.021 at X = 0.0 and then monotonically approaches the value for the fully developed Hartmann flow for the respective Hartmann numbers (see Table B-5).

A segment of the curve for M = 6 is shown in Figure 3 to indicate the rapid increase of the critical Reynolds number near the channel inlet for large Hartmann numbers. It is obvious from the behavior of the curves for lower Hartmann numbers that the M = 6 curve is expected to have a very high peak. The calculations for this curve were discontinued due to the lengthy computations arising from the numerical solution of the algebraic eigenvalue problem.

The physical reasoning behind the behavior of the axial variation of the critical Reynolds number for large Hartmann numbers is explained in section IV-D.

C. Developing Flow - Uniform Inlet Velocity Profile

For the uniform inlet velocity profile, the flow is theoretically absolutely stable to small disturbances, i.e., $R_{crit} = \infty$ at X = 0.0. Figure 4 shows the effect of channel position and Hartmann number on the neutral stability results for the developing flow induced by uniform inlet velocity profile (see Table B-6). Here again, the entrance region effects on the MHD stability characteristics are completely established with the examination of Figure 5 (see also Table B-7). The approach of the critical Reynolds number from infinity at the channel inlet to that of the fully developed Hartmann flow is again well behaved for small Hartmann numbers, say, one or less. For these small Hartmann numbers, the critical Reynolds number decreases monotonically as the axial distance increases and finally approaches the fully developed value. The curve for M = 0 in Figure 5 is taken from Chen and Sparrow (4). For larger M values, the effect is much more pronounced with the critical Reynolds number under-shooting the fully developed R_{crit} and approaching this fully developed value monotonically from below as the flow continues to develop. Obviously, the least stable flow occurs during the flow development in the entrance region. The critical wave numbers decrease very rapidly for small X and monotonically approach those of the respective fully developed Hartmann flow at large axial distances.

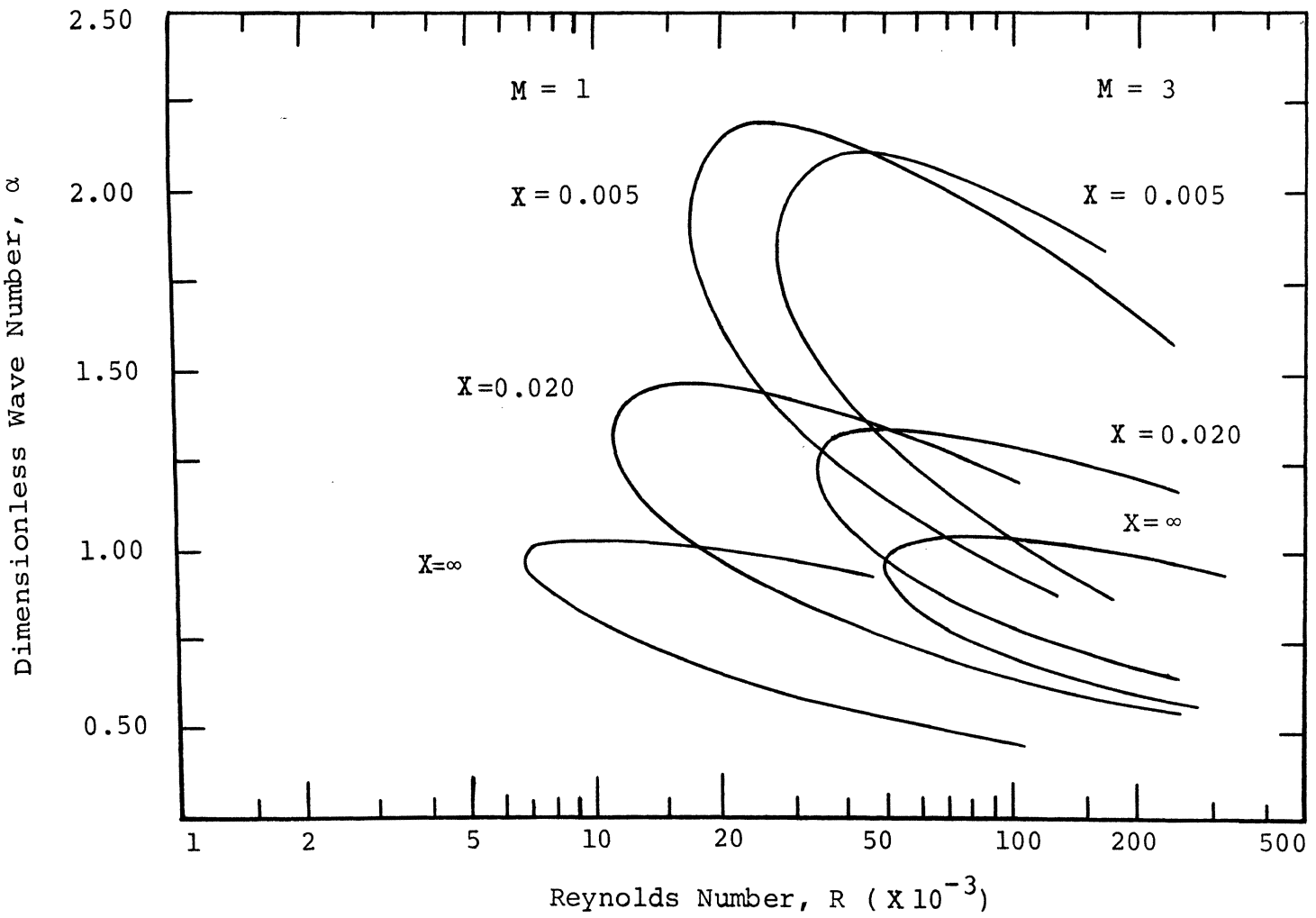

Figure 4: Representative Neutral Stability Curves for the Developing Flow, Uniform Inlet Velocity Profile

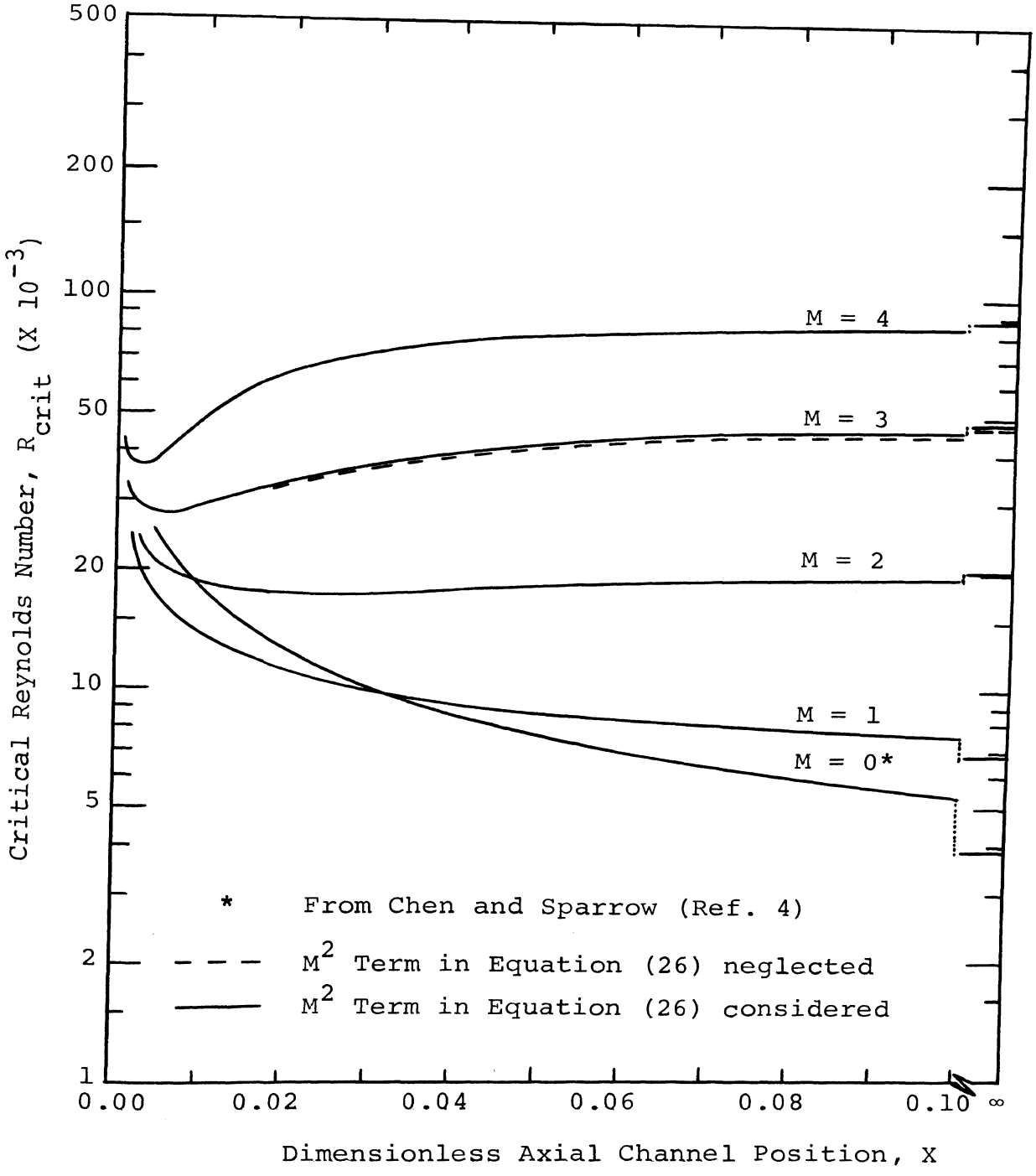

Figure 5: Variation of Critical Reynolds Number with Axial Position, Uniform Inlet Velocity Profile

The curves in Figure 5 are not complete because the numerical solution utilized requires a very large number of steps (N) or a very small step size (r) across the channel half-height in order to insure numerical accuracy. The necessity of increasing the number of steps coupled with the rather extreme behavior of the critical Reynolds number (and critical wave number) versus axial distance curve near the entrance made it very difficult to continue approaching the entrance. Nevertheless, the trends of the stability results in the entrance region are well established and all curves in Figure 5 are known to go to infinity very rapidly in a very short distance near the inlet where the numerical solution could hardly be continued.

At this point it is appropriate to direct attention to the validity of the boundary layer assumptions in the region very near the channel inlet. Numerical calculations showed that the boundary layer assumptions were still quite applicable in this region in which the stability characteristics were investigated. For example, in one case where X = 0.001 and M = 4, the $\partial^2 u/\partial x^{*2}$ term in the x-momentum equation was found to be less than one-thousandth the value of the $\partial^2 u/\partial y^{*2}$ term.

The behavior of the axial variation of the critical Reynolds number is explained in the following section.

D. The Effect of Velocity Profile on the Stability Results

Both classes of inlet velocity profiles considered in the present study undergo extensive modifications or development in the entrance region of the MHD channel. The behavior of the stability results for the fully developed Hartmann flow can be easily explained qualitatively using the basic considerations from the theory of hydrodynamic stability. However, the behavior of the axial variation of the critical Reynolds number during flow development (Figure 3 and 5) is rather surprising at first and needs further clarifications. For small Hartmann numbers (M equal to, say, one or less), the transition of the critical Reynolds number results during flow development is smooth. For larger Hartmann numbers, over-shooting and under-shooting from the fully developed critical Reynolds number for the parabolic and uniform inlet velocity profiles, respectively, become increasingly pronounced with increasing Hartmann number; an effect which is difficult to explain and which was unexpected at the onset of this investigation.

To the best knowledge of the author, neither the solution of Equation (26) by the finite difference method nor the effects of developing MHD flows on the stability characteristics have been studied previously. Therefore, the phenomenon observed in the stability results in the

entrance region which has never before been observed can be attributed to either the $M^2/i\alpha R$ term in the MHD stability equation (Equation (26)), to the effect of the volumetric MHD body force in the flow development, or possibly to a combination of these two effects.

In Figure 5, the broken line immediately under the solid line for M = 3 represents the solution of the MHD stability equation with the $M^2/i\alpha R$ term set equal to zero. Since this curve closely follows the curve from the solution of the complete equation, the presence of this term in the MHD stability equation is not responsible for the phenomenon observed in the entrance region stability results. Effort shall now be concentrated on examining the behavior of the velocity profiles in order to explain this magnetohydrodynamic stability phenomenon.

The Hartmann number squared, M^2, is the ratio of the magnetic body force to the viscous force. Thus, the magnetic force is much larger than the viscous forces for Hartmann number larger than, say, 2. Also, the magnetic or MHD field force exists only when the fluid is in motion. The actual MHD field force at any channel position can be found to be proportional to uM^2 (or WM^2).

Considering the case of uniform inlet velocity profile, the boundary layer is developing in the entrance region. Because the boundary layer must develop (non-slip

condition at the wall), x-momentum is transferred away from the walls and the velocity away from the walls increases during flow development. The transfer of x-momentum enhances the MHD body force present within the boundary layer, this body force increasing with velocity inside the boundary layer. For large Hartmann numbers, say $M > 2$, the effect is pronounced because the MHD field force is proportional to M^2. Thus in magnetohydrodynamics one might expect a rather unusual velocity profile compared with the case of pure hydrodynamics during development while the boundary layer is being created by the viscous effects in the channel.

Figure 6 shows the velocity and its first and second derivatives with respect to y for $M = 1$ and 4 and $X = 0.002$ for the uniform inlet velocity profile. The behavior of the first derivative of velocity with respect to y, W', at channel positions $y = 1.0$ and 0.9 for $M = 1$ and 4 are shown in the inset of the figure. Figure 6 establishes the effect of the magnetic field on the velocity in the developing flow region. For Hartmann numbers greater than, say, 1, the magnetic field force present in the outer areas of the developing flow boundary layer causes the velocity profile to behave in such a manner as to enhance the instability of the flow during the flow development. The velocity gradient at the wall, W',

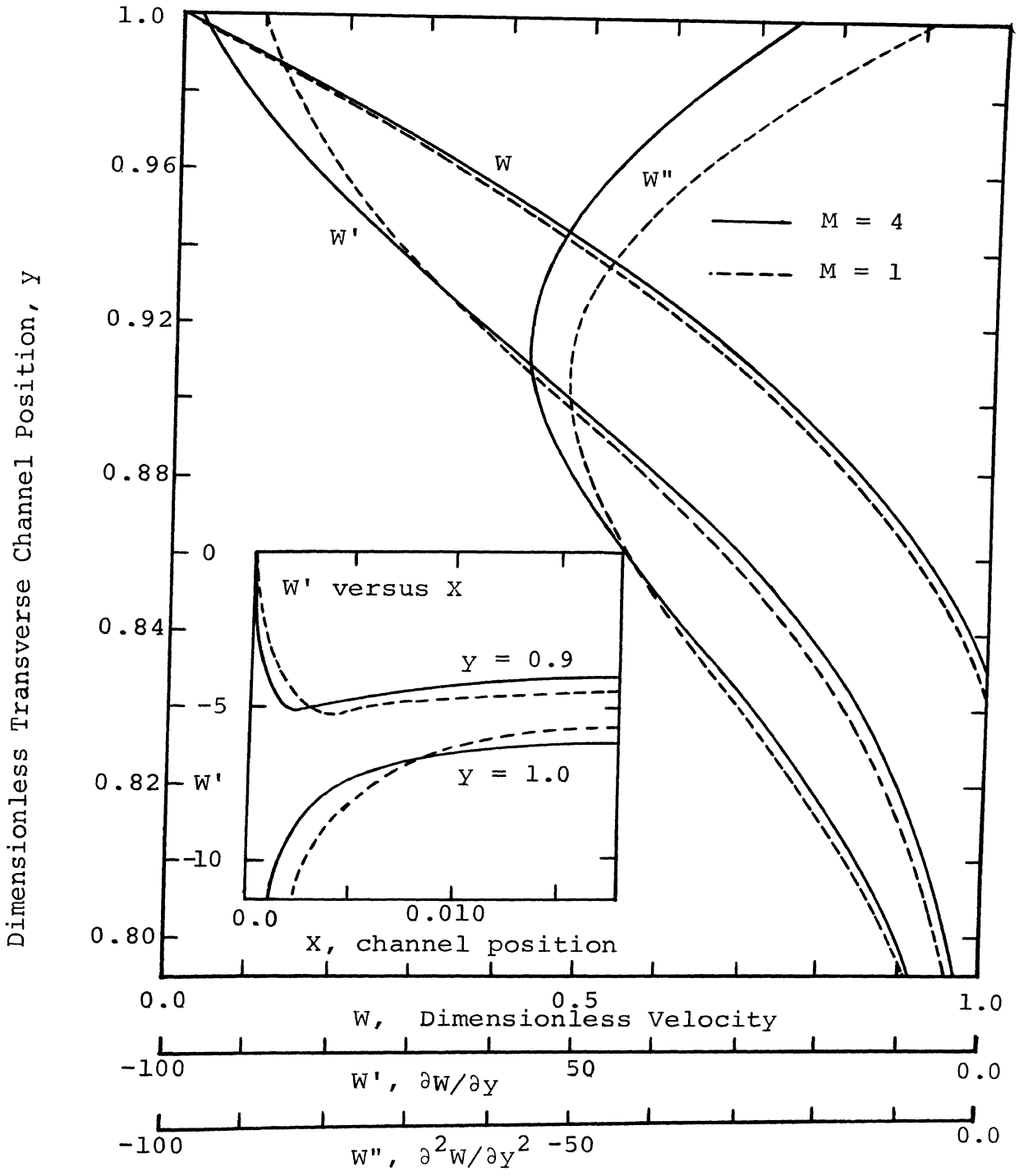

Figure 6: The Behavior of W, W', and W" Near the Wall for X = 0.002, M = 1 and 4, Uniform Inlet Velocity Profile

monotonically becomes less negative as X increases, whereas W' away from the wall (but not too near the center) decreases in value from zero at X = 0.0 to a minimum somewhere in the entrance region and then increases again to that of the fully developed flow for that y position. This phenomenon occurs only during flow development because the magnetic field force in the outer boundary layer region increases during the transfer of fluid momentum away from the wall as the boundary layer develops. The difference in the behavior of W' at various positions in the boundary layer is believed to be responsible for the under-shooting of the critical Reynolds number from that of the fully developed Hartmann flow for the reason that these derivatives, W', near and at the wall are indicators of the shape of the velocity profiles. With the information presented here and the previous qualitative discussions on hydrodynamic stability, it is obvious that the velocity profiles behave in a manner such that the stability characteristics of the developing flow induced by the uniform inlet velocity profile exhibit the unusual axial variation, as shown in Figure 5.

For the parabolic inlet velocity profile, the dimensionless centerline velocity, W, is 1.5. Thus, the core of the velocity profile where the velocity is larger than that of the fully developed Hartmann profile experiences a large retarding force, proportional to WM^2, which

encourages a rapid decrease of the velocity near the center of the channel. Thus, x-momentum of the fluid is being transferred toward the walls, and the velocity profile near the center is being rapidly flattened; because the MHD forces are largest where the velocities are largest. As x-momentum is transferred toward the walls, the MHD force in this vacinity increases because the velocity increases. However, the magnitude of the velocity gradient monotonically approaches a more negative value, and the presence of the MHD force in the outer boundary layer regions influences the flow profile so as to increase flow stability by making the velocity gradient decrease slowly in the outer boundary layer regions. Figure 7 gives the plot of velocity and its first and second derivatives with respect to y as a function of y for M = 1 and 4 at X = 0.002 for the case of parabolic inlet velocity profile. The curves in the inset of the figure show the axial variation of W' at the upper wall and at a position 10 percent of the half-channel height below the upper wall. Again, with the background previously presented, the information in Figure 7 is sufficient to establish the way the magnetic field influences the flow development which, in turn, influences the critical stability results as shown in Figure 3.

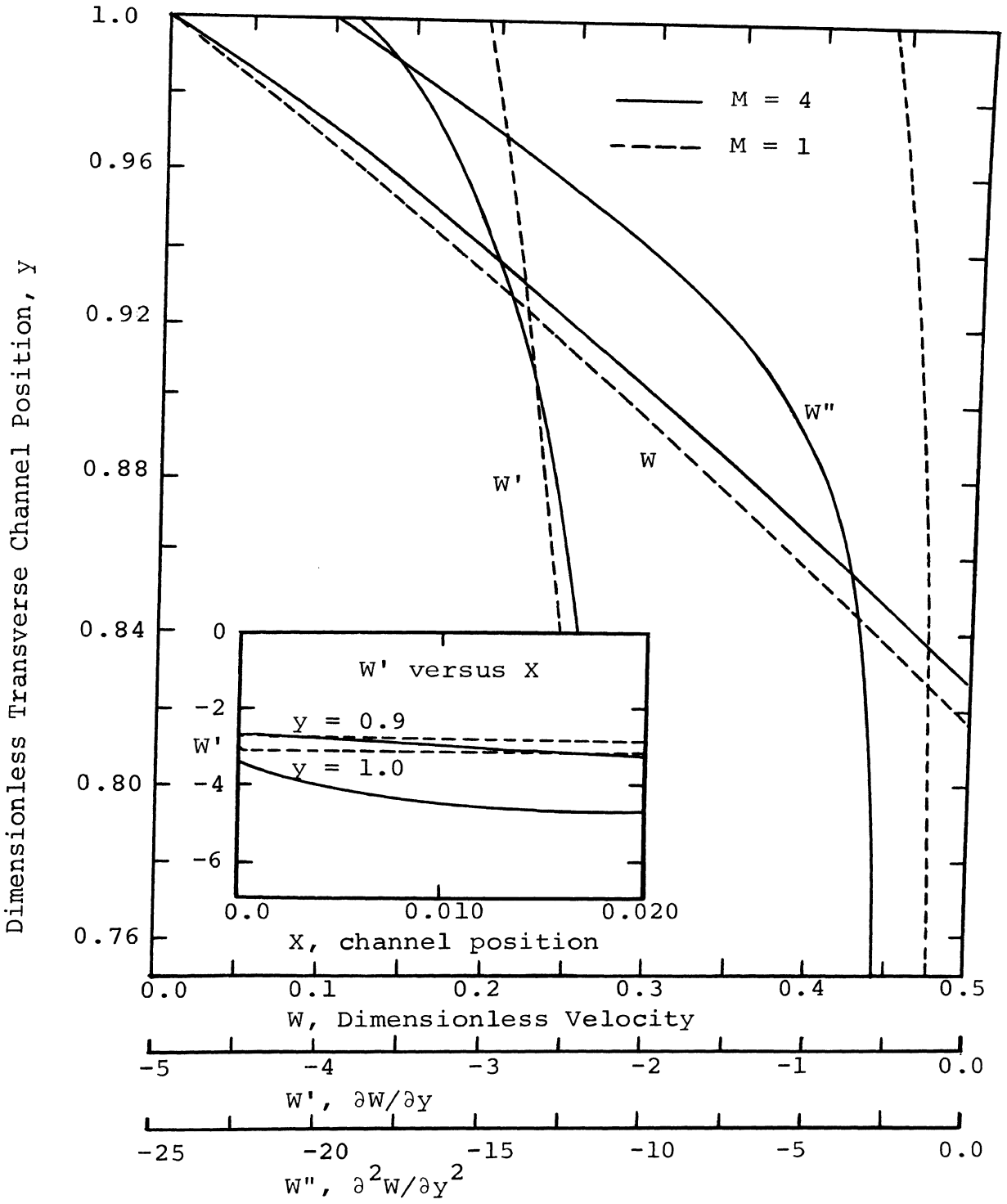

Figure 7: The Behavior of W, W', and W" Near the Wall for X = 0.002, M = 1 and 4, Parabolic Inlet Velocity Profile

As the momentum transfer is completed (i.e., when the flow is fully developed), the developing MHD forces in the outer boundary layer are reduced and the stability results monotonically approach those of the fully developed Hartmann flow from above, since the velocity profile takes on a more rounded appearance near the wall.

V. CONCLUSION

This investigation has examined the magnetohydrodynamic stability of laminar flow in the entrance region of a parallel-plate channel. By using the linear perturbation theory of hydrodynamic stability and the assumption of small magnetic Reynolds number, the governing equation of magnetohydrodynamic stability was derived. This equation was then converted into finite difference form, and a numerical solution method was employed to study the neutral stability characteristics for the fully developed Hartmann flow and the developing flows with an applied transverse magnetic field. A continuous velocity profile solution derived using linearization techniques was utilized in the stability analysis.

It is found that the numerically determined neutral stability characteristics for the fully developed Hartmann flow are in excellent agreement with the previous work of Lock (3) which used an asymptotic method of solution. The present results are believed to be more accurate than those from the analytical solution due to the more exact nature of the present investigation.

Owing to the interaction of the magnetic field with the developing flow, it is found that the magnetohydrodynamic stability characteristics in the entrance region of the channel behave in an unusual manner. For the case of uniform inlet velocity profile, the critical stability results resemble those of pure hydrodynamics for $M \leq 1$ (4) (i.e., the critical Reynolds number monotonically decreases and approaches the fully developed value at large axial distances). For $M > 1$, the critical Reynolds number tends to under-shoot the fully developed value and approach it monotonically from below at large axial distances.

For the case of parabolic inlet velocity profile, for $M \leq 1$ the critical Reynolds number tends to monotonically approach the fully developed critical Reynolds number at large axial distances from 3850 at the inlet. For $M > 1$, the critical Reynolds number over-shoots the fully developed value and approaches it monotonically from above at large axial distances.

In both cases of parabolic and uniform inlet velocity profile, the respective over-shooting and under-shooting become increasingly pronounced with increase in Hartmann number, M. The parabolic inlet flow induces a flow which is most stable during its development for $M \geq 2$ and which is most stable at the fully developed condition for $M < 2$.

The uniform inlet flow, on the other hand, induces a flow which is least stable during development for $M > 1$ and is least stable at the fully developed condition for $M \leq 1$.

VI. REFERENCES

1. Schlichting, H., Boundary Layer Theory, Part C, Sixth Edition, McGraw-Hill, New York (1968).

2. Stuart, J.T., "On the Stability of Viscous Flow Between Parallel-Plates under a Transverse Magnetic Field," Proceedings of the Royal Society of London, A 221, 189 (1954).

3. Lock, R.C., "The Stability of the Flow of an Electrically Conducting Fluid Between Parallel-Plates under a Transverse Magnetic Field," Proceedings of the Royal Society of London, A 233, 105 (1955).

4. Chen, T.S. and Sparrow, E.M., "Stability of Developing Laminar Flow in a Parallel-Plate Channel," Journal of Fluid Mechanics, 30, Part 2, 209 (1967).

5. Chen, T.S. and Sparrow, E.M., "Stability of Asymmetric Hydrodynamically Developing Channel Flows," Physics of Fluids, 13, 827 (1970).

6. Chen, T.S., "Hydrodynamic Stability of Developing Flow in a Parallel-Plate Channel," Ph.D. Thesis, Department of Mechanical Engineering, University of Minnesota (1966).

7. Chen, T.S., Personal Communications (1970).

8. Maciulaitis, A. and Loeffler, A.L. Jr., "A Theoretical Investigation of MHD Channel Entrance Flows," AIAA Journal, 2, 2100 (1964).

9. Roidt, M. and Cess, R.D., "An Approximate Analysis of Laminar Magnetohydrodynamic Flow in the Entrance Region of a Flat Duct," Journal of Applied Mechanics, Trans. ASME, 84, 171 (1962).

10. Hwang, C.L. and Fan, L.T., "A Finite-Difference Analysis of Laminar Magnetohydrodynamic Flow in the Entrance Region of a Flat Rectangular Duct," Applied Scientific Research, B 10, 329 (1963).

11. Hwang, C.L., Li, K.C., and Fan, L.T., "Magneto-hydrodynamic Channel Entrance Flow with Parabolic Velocity at the Entry," Physics of Fluids, 9, 1134 (1966).

12. Sparrow, E.M., Lin, S.H., and Lundgren, T.S., "Flow Development in the Hydrodynamic Entrance Region of Tubes and Ducts," Physics of Fluids, 7, 338 (1964).

13. Snyder, W.T., "Magnetohydrodynamic Flow in the Entrance Region of a Parallel-Plate Channel," AIAA Journal, 3, 1833 (1965).

14. Chen, G.L., "Magnetohydrodynamic Channel Flow with Non-Uniform Inlet Velocity Profiles," M.S. Thesis, University of Missouri-Rolla (1970).

15. Squire, H.B., "On the Stability for Three-Dimensional Disturbances of Viscous Fluid Flow Between Parallel Walls," Proceedings of the Royal Society, A 142, 621 (1933).

16. Grohne, D., "Über des Spektrum bei Eigenschwingungen ebener Laminarstromungen," Zeit angew. Math. Mech., 34, 344 (1954), English translation: NACA-TM 1417 (1957).

17. Thomas, L.H., "The Stability of Plane Poiseuille Flow," Physical Review, 91, 780 (1953).

18. Muller, D.E., "A Method for Solving Algebraic Equations Using an Automatic Computer," Mathematical Tables and Other Aids to Computations, 10, 208 (1956).

VII. APPENDICES

Appendix A
Derivation of the Magnetohydrodynamic Stability Equation, Equation (26)

From the text, it has been established that for two-dimensional flow, the Navier-Stokes equations of fluid motion in the x* and y* directions are, respectively,

$$\frac{\partial u}{\partial t^*} + u\frac{\partial u}{\partial x^*} + v\frac{\partial u}{\partial y^*} = \frac{\mu_m H_y}{\rho}\left(\frac{\partial H_x}{\partial y^*} - \frac{\partial H_y}{\partial x^*}\right) - \frac{1}{\rho}\frac{\partial p}{\partial x^*} + \nu\left(\frac{\partial^2 u}{\partial x^{*2}} + \frac{\partial^2 u}{\partial y^{*2}}\right) \tag{A-1}$$

$$\frac{\partial v}{\partial t^*} + u\frac{\partial v}{\partial x^*} + v\frac{\partial v}{\partial y^*} = \frac{\mu_m H_x}{\rho}\left(\frac{\partial H_y}{\partial x^*} - \frac{\partial H_x}{\partial y^*}\right) - \frac{1}{\rho}\frac{\partial p}{\partial y^*} + \nu\left(\frac{\partial^2 v}{\partial x^{*2}} + \frac{\partial^2 v}{\partial y^{*2}}\right) \tag{A-2}$$

The variables in these functions are next assumed to be composed of a main component and a superimposed, small, two-dimensional, time-dependent disturbance. The main flow is assumed to be parallel and the applied magnetic field $\overline{H}_y = H_o$, a constant. Thus, the resultant flow and magnetic fields are given by

$$
\begin{aligned}
u &= \bar{u}(y^*) + u^+(x^*,y^*,t^*) \\
v &= v^+(x^*,y^*,t^*) \\
H_x &= \bar{H}_x(y^*) + h_x{}^+(x^*,y^*,t^*) \\
H_y &= H_o + h_y{}^+(x^*,y^*,t^*) \\
p &= \bar{p}(x^*,y^*,t^*) + p^+(x^*,y^*,t^*)
\end{aligned}
\tag{A-3}
$$

where the plus (+) superscript indicates a perturbation quantity. It is postulated that the resultant flow and magnetic fields are governed by the Navier-Stokes equations as are the main flow and magnetic fields. Upon substituting Equation (A-3) into Equations (A-1) and (A-2), linearizing (neglecting the product of these small perturbations), and keeping only terms arising from the perturbations, one obtains the perturbation equations of motion:

$$
\begin{aligned}
\frac{\partial u^+}{\partial t^*} + \bar{u}\frac{\partial u^+}{\partial x^*} + v^+\frac{\partial \bar{u}}{\partial y^*} = \frac{\mu_m}{\rho}\Big(H_o\frac{\partial h^+_x}{\partial y^*} - H_o\frac{\partial h^+_y}{\partial x^*} \\
+ h^+_y\frac{\partial \bar{H}_x}{\partial y^*}\Big) - \frac{1}{\rho}\frac{\partial p^+}{\partial x^*} + \nu\Big(\frac{\partial^2 u^+}{\partial x^{*2}} + \frac{\partial^2 u^+}{\partial y^{*2}}\Big)
\end{aligned}
\tag{A-4}
$$

$$
\begin{aligned}
\frac{\partial v^+}{\partial t^*} + \bar{u}\frac{\partial v^+}{\partial x^*} = \frac{\mu_m}{\rho}\Big(\bar{H}_x\frac{\partial h^+_y}{\partial x^*} - \bar{H}_x\frac{\partial h^+_x}{\partial y^*} - h^+_x\frac{\partial \bar{H}_x}{\partial y^*}\Big) \\
- \frac{1}{\rho}\frac{\partial p^+}{\partial y^*} + \nu\Big(\frac{\partial^2 v^+}{\partial x^{*2}} + \frac{\partial^2 v^+}{\partial y^{*2}}\Big)
\end{aligned}
\tag{A-5}
$$

The equations of continuity for the perturbations are obtained in a similar manner, giving

Perturbation mass conservation

$$\frac{\partial u^+}{\partial x^*} + \frac{\partial v^+}{\partial y^*} = 0 \qquad \text{(A-6)}$$

Perturbation magnetic field conservation

$$\frac{\partial h_x^+}{\partial x^*} + \frac{\partial h_y^+}{\partial y^*} = 0 \qquad \text{(A-7)}$$

From potential theory, a stream function solution of the continuity equations may be formulated as:

Perturbation flow stream function

$$\Psi^*(x^*,y^*,t^*) = \phi^*(y^*)\ \exp[i\bar{\alpha}(x^* - \bar{c}t^*)] \qquad \text{(A-8)}$$

Perturbation magnetic stream function

$$\chi^*(x^*,y^*,t^*) = \theta^*(y^*)\ \exp[i\bar{\alpha}(x^* - \bar{c}t^*)]$$

where $\phi^*(y^*)$ and $\theta^*(y^*)$ are amplitude functions, $\bar{\alpha}$ is the dimensional wave number, $\bar{c}$ is the dimensional, complex velocity of wave propagation. These stream functions may be utilized to determine expressions for the perturbation velocities and magnetic fields. It is straightforward that

$$\begin{aligned}
u^+ &= \frac{\partial \Psi^*}{\partial y^*} = \phi^{*\prime}\ \exp[i\bar{\alpha}(x^*-\bar{c}t^*)] \\
v^+ &= -\frac{\partial \Psi^*}{\partial x^*} = -\phi^* i\bar{\alpha}\ \exp[i\bar{\alpha}(x^*-\bar{c}t^*)] \\
h_x^+ &= \frac{\partial \chi^*}{\partial y^*} = \theta^{*\prime}\ \exp[i\bar{\alpha}(x^*-\bar{c}t^*)] \\
h_y^+ &= -\frac{\partial \chi^*}{\partial x^*} = -\theta^* i\bar{\alpha}\ \exp[i\bar{\alpha}(x^*-\bar{c}t^*)]
\end{aligned} \qquad \text{(A-9)}$$

Also, one may note that the disturbance amplitude is exponentially damped with time if the imaginary component of the wave velocity has a negative value. If, of the other hand, the imaginary component of the wave velocity is positive, the disturbances amplitudes grow exponentially with time. These two cases correspond to theoretically stable and unstable flow, respectively.

Next, substituting Equation (A-9) into Equations (A-4) and (A-5) and eliminating the pressure terms by cross-differentiation, one obtains after some rearrangement

$$(\bar{u}-\bar{c})(\phi^{*\prime\prime}-\bar{\alpha}^2\phi^*) - \phi^*\bar{u}'' = \frac{\nu}{i\bar{\alpha}}(\phi^{*iv}-2\bar{\alpha}^2\phi^{*\prime\prime} + \bar{\alpha}^4\phi^*) + \frac{\mu_m H_o}{\rho i\bar{\alpha}}(\theta^{*\prime\prime\prime}-\bar{\alpha}^2\theta^{*\prime}-\theta^* i\bar{\alpha}\frac{\bar{H}_x''}{H_o} - \frac{\bar{H}_x^*}{H_o} i\bar{\alpha}^3\theta^* + i\bar{\alpha}\frac{\bar{H}_x}{H_o}\theta^{*\prime\prime}) \quad \text{(A-10)}$$

By introducing the following dimensionless variables,

$$W = \bar{u}/U,\ c = \bar{c}/U,\ X = (x^*/L)/R,\ y = y^*/L,$$
$$\alpha = \bar{\alpha}\,L,\ h = \bar{H}_x/H_o,\ \phi = \phi^*/LU,\ \theta = \theta^*/LU,$$
$$\text{and } t = t^*U/L \quad \text{(A-11)}$$

Equation (A-10) becomes

$$(W-c)(\phi''-\alpha^2\phi) - W''\phi = \frac{1}{i\alpha R}(\phi^{iv}-2\alpha^2\phi''+\alpha^4\phi) + \frac{M^2}{RR_m}[h(\theta''-\alpha^2\theta) - \theta h'' + \frac{i}{\alpha}(\alpha^2\theta'-\theta''')] \quad \text{(A-12)}$$

From the approximation of small megnetic Reynolds number (defined as $R_m = UL/\lambda$) and from order of magnitude comparisons, $h = \bar{H}_x/H_o$ is found to be quite small, of the order 10^{-6} or so, depending on the magnetic field strength and the properties of the working fluid. Thus, the small magnetic Reynolds number approximation permits the postulate that h and h" are much smaller than θ' and θ''' and can, therefore, be neglected. With this, Equation (A-12) becomes

$$(W-c)(\phi''-\alpha^2\phi)-W''\phi = \frac{1}{i\alpha R}(\phi^{iv}-2\alpha^2\phi''+\alpha^4\phi) - \frac{M^2}{RR_m} \cdot \left[\frac{i}{\alpha}(\theta'''-\alpha^2\theta')\right] \tag{A-13}$$

If one now examines the magnetic transport equation, Equation (9), it is possible to eliminate the function θ and its derivatives from Equation (A-13). The magnetic transport equations for two-dimensional flow are, in component form,

$$\frac{\partial H_x}{\partial t^*} + u\frac{\partial H_x}{\partial x^*} + v\frac{\partial H_x}{\partial y^*} - H_x\frac{\partial u}{\partial x^*} - H_y\frac{\partial u}{\partial y^*} = \lambda\frac{\partial^2 H_x}{\partial x^{*2}} + \lambda\frac{\partial^2 H_x}{\partial y^{*2}} \tag{A-14}$$

$$\frac{\partial H_y}{\partial t^*} + u\frac{\partial H_y}{\partial x^*} + v\frac{\partial H_y}{\partial y^*} - H_x\frac{\partial v}{\partial x^*} - H_y\frac{\partial v}{\partial y^*} = \lambda\frac{\partial^2 H_y}{\partial x^{*2}} + \lambda\frac{\partial^2 H_y}{\partial y^{*2}} \tag{A-15}$$

Again, introducing the perturbation equations, Equation (A-3), using linear theory, and retaining terms from perturbations, the perturbation equations for the magnetic field become

$$\frac{\partial h_x^+}{\partial t^*} + \bar{u}\frac{\partial h_x^+}{\partial x^*} + v^+\frac{\partial \bar{H}_x}{\partial y} - \bar{H}_x\frac{\partial u^+}{\partial x^*} - H_o\frac{\partial u^+}{\partial y^*} - h_y^+\frac{\partial \bar{u}}{\partial y^*} = \lambda\frac{\partial^2 h_x^+}{\partial x^{*2}} + \lambda\frac{\partial^2 h_x^+}{\partial y^{*2}} \tag{A-16}$$

$$\frac{\partial h_y^+}{\partial t^*} + \bar{u}\frac{\partial h_y^+}{\partial x^*} - \bar{H}_x\frac{\partial v^+}{\partial x^*} - H_o\frac{\partial v^+}{\partial y^*} = \lambda\frac{\partial^2 h_y^+}{\partial x^{*2}} + \lambda\frac{\partial^2 h_y^+}{\partial y^{*2}} \tag{A-17}$$

Substituting the expression for the perturbation stream functions from Equation (A-9) into Equation (A-16), one obtains the dimensional x-component equation for the magnetic disturbance as

$$h\phi^* + \frac{\phi^{*\prime}}{i\bar{\alpha}} = \frac{(\bar{u}-\bar{c})}{H_o}\theta^* - \frac{\lambda}{i\bar{\alpha}H_o}(\theta^{*\prime\prime} - \bar{\alpha}^2\theta^*) \tag{A-18}$$

In terms of the dimensionless expressions previously stated, this equation becomes

$$h\phi - \frac{i\phi'}{\alpha} = (W-c)\theta + \frac{i}{\alpha R_m}(\theta''-\alpha^2\theta) \tag{A-19}$$

If one works on the y-component equation for the magnetic disturbance, Equation (A-17), one will arrive at an equation exactly identical to Equation (A-19).

Next, the order of magnitude of the individual terms in Equation (A-19) are compared. Since h is of the order of R_m, which is quite small, it follows that

$$(W-c)\theta,\ h\phi << \frac{1}{\alpha R_m}(\theta'' - \alpha^2\theta),\ \frac{i\phi'}{\alpha}$$

Thus, Equation (A-19) can be approximated as

$$\frac{1}{\alpha R_m}(\theta'' - \alpha^2\theta) \simeq -\frac{\phi'}{\alpha} \tag{A-20}$$

or, after differentiating with respect to y once,

$$\theta''' - \alpha^2\theta' \simeq -R_m\phi'' \tag{A-21}$$

when the magnetic Reynolds number is assumed small. Finally, substitution of Equation (A-21) into Equation (A-13) gives

$$(W-c)(\phi''-\alpha^2\phi)-W''\phi = \frac{1}{i\alpha R}(\phi^{iv}-(M^2+2\alpha^2)\phi''+\alpha^4\phi) \tag{A-22}$$

which is Equation (26) in the text.

Equation (A-22) is the governing equation of magneto-hydrodynamic stability for low magnetic Reynolds number.

The small R_m approximation implies that the MHD stability equation may be of questionable validity as the

Reynolds number approaches the value of $1/R_m$. Nevertheless, the validity of the solution of Equation (A-22) depends upon the properties of the working fluid and the applied magnetic field. For Mercury, $R_m \simeq 10^{-6}$, and the solution should be valid for Reynolds number as high as 300,000.0, perhaps much higher.

In closing it is noted that Equation (A-22) reduces to

$$(W - c)(\phi'' - \alpha^2\phi) - W''\phi = \frac{1}{i\alpha R}(\phi^{iv} - 2\alpha^2\phi'' + \alpha^4\phi) \quad \text{(A-23)}$$

when the Hartmann number, M, equals zero. This reduced equation is the famous Orr-Sommerfeld equation of hydrodynamic stability.

APPENDIX B

TABULATION OF NUMERICAL RESULTS

Table B-1

The Relationship Between X and $\bar{X}$

X	$\bar{X}$, $W_o = 1.5(1-y^2)$				$\bar{X}$, $W_o = 1$			
	M				M			
	1	2	3	4	1	2	3	4
0.002	0.00282	0.00285	0.00282	0.00278	0.00517	0.00540	0.00537	0.00487
0.005	0.00648	0.00649	0.00645	0.00645	0.01171	0.01108	0.01104	0.01060
0.007	0.00876	0.00876	0.00872	0.00871	0.01524	0.01449	0.01442	0.01397
0.010	0.01204	0.01204	0.01200	0.01199	0.01980	0.01922	0.01911	0.01865
0.020	0.02240	0.02232	0.02242	0.02236	0.03356	0.03345	0.03328	0.03240
0.030	0.03210	0.03209	0.03230	0.03239	0.04567	0.04557	0.04545	0.04466
0.040	0.04151	0.04160	0.04200	0.04232	0.05682	0.05678	0.05673	0.05609
0.050	0.05074	0.05098	0.05160	0.05222	0.06735	0.06739	0.06748	0.06704
0.060	0.05986	0.06027	0.06116	0.06214	0.07746	0.07761	0.07789	0.07769
0.080	0.07790	0.07872	0.08025	0.08204	0.09687	0.09732	0.09805	0.09845
0.100	0.09581	0.09718	0.09934	0.10212	0.11564	0.11646	0.11774	0.11882

Table B-2

Neutral Stability Characteristics for the Fully Developed Hartmann Flow

α	R	c_r	α	R	c_r
		M = 1			
0.500	77307	0.1584	0.980	6804	0.3487
0.550	47618	0.1828	1.000	6937	0.3505
0.600	31387	0.2070	1.020	7298	0.3500
0.650	21939	0.2308	1.040	8352	0.3439
0.700	16137	0.2537	1.037	14000	0.3116
0.750	12431	0.2756	1.017	20000	0.2887
0.800	9997	0.2961	0.995	26000	0.2723
0.820	9275	0.3038	0.976	32000	0.2598
0.840	8664	0.3112	0.938	47000	0.2378
0.860	8151	0.3182	0.878	82000	0.2088
0.880	7726	0.3248	0.854	102000	0.1982
0.900	7380	0.3309	0.835	122000	0.1899
0.920	7111	0.3365	0.818	142000	0.1831
0.940	6920	0.3414	0.804	162000	0.1774
0.960	6812	0.3456			
		M = 2			
0.430	428795	0.1038	0.900	20576	0.2681
0.490	206302	0.1285	0.950	20576	0.2737
0.550	114240	0.1531	1.000	25553	0.2668
0.610	70311	0.1772	1.006	38000	0.2467
0.670	47280	0.2004	0.991	53000	0.2296
0.730	34294	0.2220	0.974	68000	0.2172
0.750	31313	0.2287	0.942	98000	0.1998
0.770	28815	0.2352	0.929	113000	0.1933
0.790	26725	0.2414	0.916	128000	0.1878
0.810	24984	0.2472	0.905	143000	0.1830
0.830	23549	0.2527	0.895	158000	0.1788
0.850	22377	0.2578			

Table B-2 (Continued)

			M = 3		
0.570	249570	0.1322	1.010	51751	0.2283
0.580	229859	0.1355	1.053	81000	0.2105
0.670	122274	0.1643	1.044	111000	0.1968
0.770	72735	0.1935	1.029	141000	0.1866
0.870	53918	0.2155	1.009	181000	0.1764
0.940	48845	0.2259	0.990	221000	0.1686
0.970	48751	0.2283	0.973	261000	0.1622
			M = 4		
0.600	474131	0.1182	1.139	126730	0.1946
0.700	240698	0.1451	1.142	156730	0.1862
0.800	147454	0.1692	1.136	186700	0.1794
0.880	112134	0.1853	1.127	216700	0.1736
0.960	94340	0.1976	1.117	246700	0.1689
0.990	90985	0.2010	1.096	306000	0.1607
1.020	89184	0.2036	1.077	366000	0.1543
1.060	90066	0.2053	1.059	426000	0.1491
1.100	96730	0.2042	1.043	486000	0.1447

Table B-3

Comparison of Critical Stability Characteristics for the Fully Developed Hartmann Flow

	Lock's Work (Ref.3) Analytical Solution			Present Work Numerical Solution		
M	α_{crit}	R_{crit}	$c_{r\ crit}$	α_{crit}	R_{crit}	$c_{r\ crit}$
0	1.03	4000	0.393	1.021*	3850*	0.3959*
1	0.98	7080	0.3510	0.980	6804	0.3487
2	0.93	21165	0.2844	0.923	20354	0.2718
3	0.96	51199	0.2538	0.958	48630	0.2274
4	1.04	92663	0.2370	1.034	89000	0.2046
6	1.27	194300	- -	1.246	184600	0.1853
10	1.75	417600	- -	1.720	415000	0.1707

*Numerical solution for M = 0 from Chen (6)

Table B-4

Neutral Stability Characteristics for Developing Flow, Parabolic Inlet Velocity Profile

α	R	c_r	α	R	c_r
		M = 1, X = 0.005			
0.520	50702	0.1763	0.980	4835	0.3754
0.580	29331	0.2076	1.020	4994	0.3799
0.640	18504	0.2382	1.050	8600	0.3480
0.700	12579	0.2680	1.060	8618	0.3490
0.760	9124	0.2963	1.003	17200	0.2998
0.820	7028	0.3226	0.965	25800	0.2734
0.880	5748	0.3461	0.920	40000	0.2468
0.940	5028	0.3657	0.877	60000	0.2242
		M = 1, X = 0.020			
0.360	444642	0.0946	1.028	12000	0.3219
0.460	107312	0.1428	0.979	24000	0.2714
0.560	38740	0.1928	0.947	34000	0.2555
0.660	18218	0.2421	0.992	44000	0.2407
0.760	10475	0.2881	0.901	54000	0.2294
0.860	7181	0.3278	0.866	75000	0.2122
0.890	6649	0.3379	0.836	100000	0.1982
0.920	6279	0.3467	0.812	125000	0.1878
0.950	6076	0.3539	0.793	150000	0.1797
0.990	6161	0.3594	0.777	175000	0.1732
1.030	7610	0.3513			
		M = 3, X = 0.005			
0.560	127606	0.1549	0.764	170000	0.1657
0.620	85788	0.1765	0.760	186687	0.1621
0.680	65791	0.1944	0.754	210000	0.1577
0.740	61827	0.2039	0.745	250000	0.1513
0.776	90000	0.1912	0.740	275965	0.1478
0.773	130000	0.1763	0.680	633551	0.1211

Table B-4 (Continued)

M = 3, X = 0.020					
0.480	414334	0.1109	0.900	99733	0.1950
0.500	336639	0.1181	0.901	103500	0.1909
0.520	277586	0.1251	0.897	133500	0.1807
0.560	196453	0.1391	0.893	153000	0.1753
0.620	128363	0.1589	0.887	173000	0.1705
0.680	92489	0.1769	0.881	193000	0.1663
0.740	73248	0.1921	0.869	230000	0.1598
0.800	64669	0.2030	0.858	270000	0.1539
0.820	63940	0.2050	0.847	310000	0.1491
0.880	73589	0.2039	0.837	350000	0.1449

Table B-5

Variation of the Critical Wave and Reynolds Numbers with Axial Position, Parabolic Inlet Velocity Profile

	M = 1.0		M = 2.0		M = 3.0		M = 4.0	
	α_{crit}	R_{crit}	α_{crit}	R_{crit}	α_{crit}	R_{crit}	α_{crit}	R_{crit}
0.000	1.021	3850	1.021	3850	1.021	3850	1.021	3850
0.001	-	-	-	-	-	-	0.652	31700
0.002	1.005	4210	0.945	6415	0.807	17995	0.607	179900
0.003	-	-	-	-	-	-	0.635	203500
0.005	0.976	4975	0.866	11935	0.719	59920	0.670	206700
0.007	-	-	-	-	-	-	0.718	194000
0.010	0.974	5475	0.838	17415	0.753	69960	0.764	169000
0.020	0.964	6045	0.855	20090	0.825	63700	0.867	137250
0.030	-	-	0.868	20650	-	-	0.931	115900
0.040	0.964	6440	-	-	0.880	56040	0.953	106220
0.060	0.968	6590	0.895	20750	0.907	53450	0.998	96600
0.080	-	-	-	-	0.934	51100	-	-
0.010	0.969	6701	0.908	20550	0.947	50600	1.030	90250
∞	0.960	6809	0.923	20354	0.958	48630	1.034	89000

Table B-6

Neutral Stability Characteristics for Developing Flow, Uniform Inlet Velocity Profile

α	R	c_r	α	R	c_r
		M = 1, X = 0.005			
0.920	106827	0.1853	1.940	17438	0.3273
1.070	60214	0.2188	2.040	17807	0.3295
1.170	44795	0.2387	2.213	25000	0.3146
1.270	35144	0.2567	2.142	45000	0.2819
1.370	28835	0.2727	1.997	75000	0.2546
1.470	24562	0.2869	1.889	105000	0.2377
1.570	21640	0.2991	1.807	135000	0.2256
1.640	20164	0.3065	1.742	165000	0.2163
1.740	18655	0.3155	1.688	195000	0.2088
1.840	17763	0.3225			
		M = 1, X = 0.020			
0.530	282383	0.1222	1.360	11282	0.3348
0.630	115400	0.1581	1.469	21300	0.3047
0.730	58368	0.1923	1.426	32300	0.2802
0.830	34499	0.2257	1.382	43300	0.2634
0.930	23006	0.2555	1.304	68000	0.2390
1.030	16935	0.2818	1.247	93000	0.2231
1.129	13600	0.3038	1.196	123000	0.2096
1.200	12192	0.3168	1.156	153000	0.1995
1.260	11490	0.3256			
		M = 3, X = 0.005			
1.000	119431	0.1886	1.640	31032	0.2845
1.075	91595	0.2038	1.740	28922	0.2924
1.140	74996	0.2162	1.840	27871	0.2980
1.240	57782	0.2336	1.940	27965	0.3011
1.340	46715	0.2492	2.099	60000	0.2650
1.440	39357	0.2629	2.039	80000	0.2501
1.540	34370	0.2747	1.982	100000	0.2389

Table B-6 (Continued)

M = 3, X = 0.020					
0.650	237782	0.1401	1.280	34279	0.2658
0.700	168344	0.1552	1.320	36493	0.2647
0.800	95675	0.1838	1.351	51000	0.2491
0.900	62318	0.2098	1.343	66000	0.2364
1.000	45481	0.2323	1.322	86000	0.2235
1.080	38098	0.2471	1.283	120000	0.2078
1.016	34120	0.2585	1.242	160000	0.1949
1.220	33096	0.2640	1.213	195000	0.1864
1.240	32466	0.2663	1.184	235000	0.1787

Table B-7

Variation of the Critical Wave and Reynolds Numbers with Axial Position, Uniform Inlet Velocity Profile

X	M = 1		2		3		4	
	α_{crit}	R_{crit}	α_{crit}	R_{crit}	α_{crit}	R_{crit}	α_{crit}	R_{crit}
0.001	-	-	-	-	-	-	3.880	40730
0.002	2.855	24770	-	-	2.695	30670	2.771	37190
0.003	-	-	2.260	23775	-	-	2.298	37120
0.004	-	-	-	-	2.058	28030	-	-
0.005	1.948	17410	1.950	21050	1.885	27700	1.851	39600
0.006	-	-	-	-	1.763	27690	-	-
0.007	-	-	1.738	19700	-	-	1.630	42930
0.010	1.586	13885	1.545	18600	1.485	28700	1.444	48140
0.020	1.384	11125	1.276	17750	1.224	33090	1.216	62320
0.030	1.221	10025	1.161	17610	1.124	37100	-	-
0.040	1.153	9322	-	-	-	-	1.096	77140
0.050	1.115	8830	1.051	18370	1.039	42100	-	-
0.060	1.079	8470	-	-	-	-	1.060	82980
0.080	1.025	8060	0.984	19280	0.985	46055	-	-
0.010	1.018	7670	-	-	0.977	47200	1.038	86600
∞	0.980	6804	0.980	20354	0.958	48630	1.034	89000

VIII. VITA

The author, Thomas Eldon Eaton, was born on November 27, 1948, in Ironton, Missouri. He received his primary and secondary education in the public schools of Iron County, Missouri. He received a Bachelor of Science degree in Mechanical Engineering in January, 1970, from the University of Missouri-Rolla.

He began his graduate work at the University of Missouri-Rolla in September, 1969, as a dually-enrolled student and attained graduate student status in January, 1970. He has held a National Science Foundation Traineeship for the period February, 1970 to August, 1970.